Atmospheric
Chemistry
and Physics
Discussions

1 **The atmospheric impacts of monoterpene ozonolysis on**

2 **global stabilised Criegee intermediate budgets and SO$_2$**

3 **oxidation: experiment, theory and modelling**

4

5 **Mike J. Newland[1,3], Andrew R. Rickard[2,3], Tomás Sherwen[3], Mathew J. Evans[2,3],**

6 **Luc Vereecken[4,5], Amalia Muñoz[6], Milagros Ródenas[6], William J. Bloss[1]**

7 [1]{University of Birmingham, School of Geography, Earth and Environmental Sciences,
8 Birmingham, UK}

9 [2]{National Centre for Atmospheric Science (NCAS), University of York, York, UK}

10 [3]{Wolfson Atmospheric Chemistry Laboratories, Department of Chemistry, University of
11 York, York, UK}

12 [4]{Max Planck Institute for Chemistry, Atmospheric Sciences, Hahn-Meitner-Weg 1, Mainz,
13 Germany}

14 [5]{Institute for Energy and Climate Research, Forschungszentrum Jülich GmbH, Jülich,
15 Germany}

16 [6]{Fundación CEAM, EUPHORE Laboratories, Avda/Charles R. Darwin 14. Parque
17 Tecnologico, Valencia, Spain}

18 Correspondence to: M. J. Newland (mike.newland@york.ac.uk)

19   A. R. Rickard (andrew.rickard@york.ac.uk)

20

21 **Abstract**

22 The gas-phase reaction of alkenes with ozone is known to produce stabilised Criegee
23 intermediates (SCIs). These biradical/zwitterionic species have the potential to act as
24 atmospheric oxidants for trace pollutants such as SO$_2$, enhancing the formation of sulfate
25 aerosol with impacts on air quality and health, radiative transfer and climate. However, the
26 importance of this chemistry is uncertain as a consequence of limited understanding of the
27 abundance and atmospheric fate of SCIs. In this work we apply experimental, theoretical and
28 numerical modelling methods to quantify the atmospheric impacts, abundance, and fate, of

Atmospheric
Chemistry
and Physics
Discussions

1   the structurally diverse SCIs derived from the ozonolysis of monoterpenes, the second most

2   abundant group of unsaturated hydrocarbons in the atmosphere. We have investigated the

3   removal of SO_2 by SCI formed from the ozonolysis of three monoterpenes (α-pinene, β-

4   pinene and limonene) in the presence of varying amounts of water vapour in large-scale

5   simulation chamber experiments. The SO_2 removal displays a clear dependence on water

6   vapour concentration, but this dependence is not linear across the range of $[H_2O]$ explored. At

7   low $[H_2O]$ a strong dependence of SO_2 removal on $[H_2O]$ is observed, while at higher $[H_2O]$

8   this dependence becomes much weaker. This is interpreted as being caused by the production

9   of a variety of structurally (and hence chemically) different SCI in each of the systems

10   studied, each displaying different rates of reaction with water and of unimolecular

11   rearrangement/decomposition. The determined rate constants, $k(SCI+H_2O)$, for those SCI that

12   react primarily with H_2O range from $4 - 310 \times 10^{-15}$ cm^3 s^{-1}. For those SCI that predominantly

13   react unimolecularly, determined rates range from $130 - 240$ s^{-1}. These values are in line with

14   previous results for the (analogous) stereo-specific SCI system of *syn*/*anti*-CH_3CHOO. The

15   experimental results are interpreted through theoretical studies of the SCI unimolecular

16   reactions and bimolecular reactions with H_2O, characterised for α-pinene and β-pinene at the

17   M06-2X/aug-cc-pVTZ level of theory. The theoretically derived rates agree with the

18   experimental results within the uncertainties. A global modelling study, applying the

19   experimental results within the GEOS-Chem chemical transport model, suggests that > 98 %

20   of the total monoterpene derived global SCI burden is comprised of SCI whose structure

21   determines that they react slowly with water, and whose atmospheric fate is dominated by

22   unimolecular reactions. Seasonally averaged boundary layer concentrations of monoterpene-

23   derived SCI reach up to 1.2×10^4 cm^{-3} in regions of elevated monoterpene emissions in the

24   tropics. Reactions of monoterpene derived SCI with SO_2 account for < 1 % globally but may

25   account for up to 50 % of the gas-phase SO_2 removal over areas of tropical forests, with

26   significant localised impacts on the formation of sulfate aerosol, and hence the lifetime and

27   distribution of SO_2.

28

29   **1   Introduction**

30   Chemical oxidation processes in the atmosphere exert a major influence on atmospheric

31   composition, leading to the removal of primary emitted species, and the formation of

32   secondary products. In many cases either the emitted species or their oxidation products

Atmospheric
Chemistry
and Physics
Discussions

1 negatively impact air quality and climate (e.g. ozone, which is also a potent greenhouse gas).

2 These reactions can also transform gas-phase species to the condensed phase, forming

3 secondary aerosol that again can be harmful to health and can both directly and indirectly

4 influence radiative transfer and hence climate (e.g. SO_2 oxidation leading to the formation of

5 sulfate aerosol).

6 Tropospheric gas-phase oxidants include the OH radical, ozone, the NO_3 radical, and halogen

7 atoms. Stabilised Criegee intermediates (SCIs), or carbonyl oxides, have been identified

8 as another potentially important oxidant in the troposphere (*e.g.* Cox and Penkett, 1971;

9 Mauldin et al., 2012). SCIs are thought to be formed in the atmosphere predominantly

10 from the reaction of ozone with unsaturated hydrocarbons, though other processes may

11 be important under certain conditions, e.g. alkyl iodide photolysis (Gravestock et al.,

12 2010), dissociation of the DMSO peroxy radical (Asatryan and Bozzelli, 2008).

13 Laboratory experiments and theoretical calculations have shown SCI to oxidise SO_2 (*e.g.*

14 Cox and Penkett, 1971; Welz et al., 2012; Taatjes et al., 2013), organic (Welz et al.,

15 2014) and inorganic (Foreman et al., 2016) acids (Vereecken et al., 2017), and a number

16 of other important trace gases found in the atmosphere, as well as forming adducts with

17 NO_2 (Taatjes et al., 2014; Vereecken et al., 2017; Caravan et al., 2017). Measurements in

18 a boreal forest (Mauldin et al., 2012) and at a coastal site (Berresheim et al., 2014) have

19 both identified a 'missing' process (in addition to reaction with OH) oxidising SO_2 to

20 H_2SO_4, potentially arising from SCI reactions.

21 Here, we present results from a series of experimental studies into SCI formation and

22 reactions, carried out under atmospheric boundary layer conditions in the European

23 Photochemical Reactor facility (EUPHORE), Valencia, Spain. We examine the ozonolysis of

24 three monoterpenes with very different structures (and hence reactivities with OH and ozone):

25 α-pinene (with an endocyclic double bond), β-pinene (with an exocyclic double bond) and

26 limonene (with both an endo and exo cyclic double bond). We observe the removal of SO_2 in

27 the presence of each alkene-ozone system as a function of water vapour concentration. This

28 allows us to derive relative SCI kinetics for reaction with H_2O, SO_2, and unimolecular

29 decomposition. Further, we calculate absolute unimolecular rates and bimolecular reaction

30 rates with H_2O for all α-pinene and β-pinene derived SCI at the M06-2X/aug-cc-pVTZ level

31 of theory. A global modelling study, using the GEOS-Chem global chemical transport model,

Atmospheric
Chemistry
and Physics
Discussions

1   is performed to assess global and regional impacts of the chemical kinetics of monoterpene

2   SCI determined in this study.

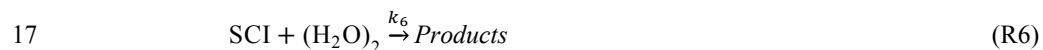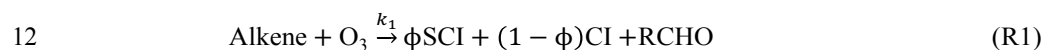3   **1.1   Stabilised Criegee Intermediate Kinetics**

4   Ozonolysis of an unsaturated hydrocarbon produces a primary ozonide that rapidly

5   decomposes to yield pairs of Criegee intermediates (CIs) and carbonyls (Johnson and

6   Marston 2008). The population of CIs are formed with a broad internal energy

7   distribution giving both chemically activated and stabilised forms. Chemically activated

8   CIs may undergo collisional stabilisation to an SCI, unimolecular decomposition or

9   isomerisation. SCIs can have sufficiently long lifetimes to undergo bimolecular reactions

10   (Scheme 1).

11   The predominant atmospheric fate for the simplest SCI, CH_2OO, is reaction with water

12   vapour (likely with the dimer (($H_2O)_2$)) (e.g. Berndt et al., 2014; Newland et al., 2015a;

13   Chao et al., 2015; Lewis et al., 2015; Lin et al., 2016). For larger SCI, both experimental

14   (Taatjes et al., 2013; Sheps et al., 2014; Newland et al., 2015a; Huang et al., 2015) and

15   theoretical (Kuwata et al., 2010; Anglada et al., 2011; Anglada and Sole, 2016) studies

16   have shown that their kinetics, in particular reaction with water, are highly structure

17   dependent. The significant double bond character exhibited in the zwitterionic

18   configurations of mono-substituted SCI leads to two distinct chemical forms: *syn*-SCI

19   (*i.e.* those where an alkyl-substituent group is on the same side as the terminal oxygen of

20   the carbonyl oxide moiety)), and *anti*-SCI (*i.e.* with the terminal oxygen of the carbonyl

21   oxide moiety on the same side as a hydrogen group). The two conformers of CH_3CHOO,

22   which are both mono-substituted, display these properties. This difference in conformer

23   reactivities has been predicted theoretically (Ryzhkov and Ariya, 2004, Kuwata et al.,

24   2010; Anglada et al., 2011; Lin et al., 2016) and was subsequently confirmed

25   experimentally (Taatjes et al., 2013; Sheps et al., 2014) for the two CH_3CHOO

26   conformers. The significantly faster reaction of *anti*-CH_3CHOO with water is driven by

27   the higher potential energy of this isomer, while more stable SCI, with a methyl group in

28   *syn*-position, such as *syn*-CH_3CHOO or $(CH_3)_2COO$, react orders of magnitude more

29   slowly with water.

30   SCI can also undergo unimolecular isomerisation/decomposition in competition with

31   bimolecular reactions. This is likely to be a significant atmospheric sink for *syn*-SCI because

Atmospheric
Chemistry
and Physics
Discussions

1   of their slow reaction with water vapour (e.g. Huang et al., 2015). Unimolecular reactions of

2   *syn*-CI/SCI are dominated by a 1,4-H-shift, forming a vinyl hydroperoxide (VHP)

3   intermediate (Niki et al., 1987; Rickard et al., 1999; Martinez and Herron, 1987; Johnson and

4   Marston, 2008; Kidwell et al., 2016). Decomposition of the VHP formed in this process is an

5   important non-photolytic source of OH, HO_2, and RO_2 in the atmosphere (Niki et al.,

6   1987; Alam et al., 2013; Kidwell et al., 2016), which can also lead to secondary organic

7   aerosol formation (Ehn et al., 2014). Unimolecular reactions of the *anti*-CI/SCI are

8   thought to be dominated by a 1,3-ring closure, the "acid/ester channel", in which the

9   CI/SCI decomposes, through a rearrangement to a dioxirane intermediate, producing a

10 range of daughter products and contributing to the observed overall HO_x radical yield

11 (Kroll et al., 2002; Johnson and Marston, 2008; Alam et al., 2013).

12 $$\text{Alkene} + O_3 \xrightarrow{k_1} \phi\text{SCI} + (1-\phi)\text{CI} + \text{RCHO} \tag{R1}$$

13 $$\text{SCI} + SO_2 \xrightarrow{k_2} SO_3 + \text{RCHO} \tag{R2}$$

14 $$\text{SCI} + H_2O \xrightarrow{k_3} Products \tag{R3}$$

15 $$\text{SCI} \xrightarrow{k_d} Products \tag{R4}$$

16 $$\text{SCI} + acid \xrightarrow{k_5} Products \tag{R5}$$

17 $$\text{SCI} + (H_2O)_2 \xrightarrow{k_6} Products \tag{R6}$$

18 Decomposition of the simplest SCI, CH_2OO, is slow (< 10 s^{-1}) and is not likely to be an

19 important sink in the troposphere (e.g. Newland et al., 2015a; Chhantyal-Pun et al., 2015).

20 This decomposition occurs primarily via rearrangement through a 'hot' acid species, which

21 represents the lowest accessible decomposition channel (Gutbrod et al., 1996; Alam et al.,

22 2011; Chen et al., 2016). However, recently determined unimolecular reaction rates of larger

23 *syn*-SCI are considerably faster. Newland et al. (2015a) reported unimolecular reaction rate

24 constants for *syn*-CH_3CHOO of 348 ($\pm$ 332) s^{-1} and for $(CH_3)_2COO$ of 819 ($\pm$ 190) s^{-1}

25 (assuming $k(syn\text{-}CH_3CHOO+SO_2)$ = 2.9 × 10^{-11} cm^3 s^{-1} (Sheps et al., 2014) and

26 $k((CH_3)_2COO+SO_2)$ = 1.3 × 10^{-10} cm^3 s^{-1} (Huang et al., 2015), respectively). Smith et al.

27 (2016) measured the unimolecular decomposition rate of $(CH_3)_2COO$ to be 269 ($\pm$ 82) s^{-1} at

28 283 K increasing to 916 ($\pm$ 56) s^{-1} at 323 K, suggesting the rate to be fast and highly

29 temperature dependent. Novelli et al. (2014), estimated a significantly slower decomposition

Atmospheric
Chemistry
and Physics
Discussions

1   rate for s*yn*-CH$_3$CHOO of 20 (3-30) s^{-1} from direct observations of OH formation, while

2   Fenske et al. (2000), estimated the decomposition rate of CH$_3$CHOO (i.e. a mix of *syn* and

3   *anti* conformers) produced from ozonolysis of *trans*-but-2-ene to be 76 s^{-1} (accurate to within

4   a factor of three).

5

6   **1.2   Monoterpene Ozonolysis**

7   Monoterpenes are volatile organic compounds (VOCs) with the general formula C$_{10}$H$_{16}$,

8   which are emitted by a wide range of vegetation, particularly from boreal forests. Total global

9   monoterpene emissions are estimated to be 95 (± 3) Tg yr^{-1} (Sindelarova et al., 2014) -

10   roughly 13 % of total non-methane biogenic VOC emissions. Monoterpene emissions are

11   dominated by α-pinene, which accounts for roughly 34 % of the total global emissions, while

12   β-pinene and limonene account for 17 % and 9 % respectively (Sindelarova et al., 2014).

13   Monoterpenes (mainly α-pinene and limonene) are also present in indoor environments, in

14   significant amounts where cleaning products and air fresheners are in routine use (on the

15   order of 100s of ppbv) (e.g. Singer et al., (2006); Sarwar and Corsi, (2007)), where their

16   ozonolysis products can affect indoor chemistry and health (*e.g.* Rossignol et al., (2013);

17   Shallcross et al., (2014)).

18   Monoterpenes are highly reactive due to the presence of (often multiple) double bonds. The

19   oxidation of monoterpenes yields a wide range of multi-functional gas-phase and aerosol

20   products. This process can be initiated by OH and NO$_3$ radicals or by O$_3$, with ozonolysis

21   having been shown to be particularly efficient at generating low volatility products that can

22   form SOA, even in the absence of sulfuric acid (e.g. Ehn et al., 2014; Kirkby et al., 2016).

23   These highly oxygenated secondary products have received considerable attention in recent

24   years because of their role in affecting the climate through absorption and scattering of solar

25   radiation (the direct aerosol effect). They can also increase cloud condensation nuclei

26   concentrations, which can change cloud properties and lifetimes (the indirect aerosol effect).

27   They have also been shown to have a wide range of deleterious effects on human health (e.g.

28   Pöschl and Shiraiwa, 2015).

29   The ozonolysis reaction for monoterpenes is expected to follow a similar initial process to

30   that of smaller alkenes, with cyclo-addition at a double bond giving a primary ozonide (POZ),

31   followed by rapid decomposition of the POZ to yield a CI and a carbonyl (Scheme 1).

Atmospheric
Chemistry
and Physics
Discussions

1   Stabilisation of the large POZs formed in monoterpene ozonolysis is expected to be

2   negligible (Nguyen et al., 2009). However, a major difference in ozonolysis at endocyclic

3   bonds is that, on decomposition of the POZ, the carbonyl oxide and carbonyl moieties are

4   tethered as part of the same molecule, providing the potential for further interaction of the

5   two. These can react together to form secondary ozonides (SOZ), which may be stable for

6   several hours (Beck et al., 2011). However, while this has been shown to be potentially the

7   major fate in the atmosphere for SCI derived from sesquiterpenes ($C_{15}H_{24}$) (e.g. Nguyen et al.,

8   2009b; Beck et al., 2011; Yao et al., 2014), formation of SOZ is predicted to be small for

9   monoterpene derived SCI because of the high ring strain caused by the tight cyclisation (e.g.

10   Nguyen et al., 2009b). Chuong et al. (2004) predicted formation of a SOZ to become the

11   dominant atmospheric fate for SCI formed in the ozonolysis of endo-cyclic alkenes with a

12   carbon number between 8 and 15, while Vereecken and Francisco (2012) suggested that

13   internal SOZ formation is likely to be limited to product rings containing six or more carbons

14   due to ring strain.

15   No studies have yet directly determined the reaction rates of the large SCI produced from

16   monoterpene ozonolysis with SO_2 (or any other trace gases). This is owing to the

17   complexities of synthesizing and measuring large SCI. However, Ahrens et al. (2014)

18   concluded that the reaction of the C9-SCI formed in β-pinene ozonolysis with SO_2 is as fast

19   as that determined by Welz et al. (2012) and Taatjes et al. (2013) for CH_2OO and CH_3CHOO

20   respectively (ca. 4×10^{-11} cm^3 s^{-1}) by fitting to the decay of SO_2 in the presence of the

21   ozonolysis reaction. Mauldin et al. (2012) calculated significantly slower reaction rates for an

22   additional oxidant (assumed to be SCI) derived from α-pinene and limonene ozonolysis, with

23   k(SCI+SO_2) determined to be 6×10^{-13} cm^3 s^{-1} and 8×10^{-13} cm^3 s^{-1} for α-pinene and limonene

24   derived SCI respectively. However, it seems likely that the rates calculated by Mauldin et al.

25   (2012) may be substantially underestimated due to the assumption of a very long SCI lifetime

26   (0.2 s) in experiments that were performed at 50 % RH. The calculated rates scale linearly

27   with SCI lifetime and based on reaction rates of smaller SCI with H_2O (reported since the

28   Mauldin et al. work, e.g. Taatjes et al., 2013) it seems likely that the lifetime of the SCI in

29   their experiments would have been more like $0.1 - 2 \times 10^{-2}$ s, increasing the calculated rate

30   constants by more than an order of magnitude, bringing them into much closer agreement

31   with the rates reported by Ahrens et al. (2014).

32   Unimolecular reactions of the monoterpene SCI are expected to proceed rapidly through the

33   VHP route if a hydrogen is available for a 1,4 H-shift. Those SCI that cannot undergo this

Atmospheric
Chemistry
and Physics
Discussions

Open Access

1   rearrangement may undergo unimolecular reactions via the formation of the dioxirane

2   intermediate, but this is expected to be a much slower process (Nguyen et al., 2009). In

3   contrast to smaller SCI, it has been observed experimentally, and predicted theoretically, that

4   the VHP route will mainly lead to rearrangement to an acid (also yielding an OH radical)

5   rather than decomposition of the molecule (e.g. Ma et al., 2008, Ma and Marston, 2008). As

6   for the smaller alkenes, monoterpene ozonolysis has been shown to be a source of HO_x (e.g.

7   Paulson et al., 1997; Alam et al., 2013), predominantly via the VHP rearrangement. The

8   MCMv3.3.1 (Jenkin et al., 2015) applies OH yields of 0.80, 0.35 and 0.87 for α-pinene, β-

9   pinene and limonene respectively.

1.2.1 α-pinene derived SCI

11   Decomposition of the α-pinene POZ yields four different C_{10} Criegee intermediates (Scheme

12   2: CI-1a, 1b, 2a, 2b), with the carbonyl oxide moiety at one end and a carbonyl group at the

13   other. Here, CI-1 is a mono-substituted CI for which both *syn* (1a) and *anti* (1b) conformers

14   exist, while the other, CI-2, is di-substituted, for which two *syn*-conformers (2a and 2b) exist.

15   Ma et al. (2008) infer a relative yield of 50 % for the two basic CI formed, based on the

16   observation that norpinonic acid yields from the ozonolysis of α-pinene and an enone, which

17   upon ozonolysis yields CI-1, are almost indistinguishable.

18   The total SCI yield from α-pinene was determined to be 0.15 (± 0.07) by Sipilä et al. (2014)

19   in indirect experiments measuring the production of H_2SO_4 from SO_2 oxidation in the α-

20   pinene ozonolysis system. Drozd and Donahue (2011) also determined a total SCI yield of

21   about 0.15 at 740 Torr, from measuring the loss of hydrofluoroacetone in ozonolysis

22   experiments in a high pressure flow system. The MCMv3.3.1 (Jenkin et al., 1997; Saunders et

23   al., 2003; Jenkin et al., 2015) applies a value of 0.20 based on stabilisation of only the mono-

24   substituted CI-1.

1.2.2 β-pinene derived SCI

26   β-pinene ozonolysis yields two distinct conformers of the nopinone C9-CI (Scheme 3: CI-3

27   and CI-4), which differ in orientation of the carbonyl oxide group, and CH_2OO. CI-3 and CI-4

28   are formed in roughly equal proportions with very little inter-conversion between the two

29   (Nguyen et al., 2009). The difference in the chemical behaviour of CI-3 and CI-4, which were

30   often not distinguished in earlier studies, arises from the inability of the carbon attached to the

31   four-membered ring to undergo the 1,4-H-shift that allows unimolecular decomposition via

Atmospheric
Chemistry
and Physics
Discussions
Open Access
EGU

1   the VHP channel. This was noted in Rickard et al. (1999) as being a reason for the

2   considerably lower OH yield (obtained via the VHP route) from β-pinene ozonolysis

3   compared to that of α-pinene. This difference leads to contrasting unimolecular

4   decomposition rates for the two CI, with Nguyen et al. (2009) predicting a loss rate of *ca.* 50

5   s^{-1} for CI-3 (via a VHP) and *ca.* 1 s^{-1} for CI-4 (via ring closure to a dioxirane). This result is

6   qualitatively consistent with the experimental work of Ahrens et al. (2014), who determine a

7   ratio of 85:15 for the abundance of SCI-4:SCI-3 about 10 s after the initiation of the

8   ozonolysis reaction, as a consequence of the much faster decomposition rate of SCI-3. Thus

9   the potential for bimolecular reactions to compete with decomposition of SCI-3 and SCI-4 in

10   the atmosphere is very different.

11   Nguyen et al. (2009) theoretically calculate a total SCI yield from β-pinene ozonolysis of 42

12   %, consisting of 16.2 % SCI-3, 20.6 % SCI-4, and 5.1 % CH_2OO. Ahrens et al. (2014)

13   assume an equal yield of CI-3 and CI-4 (45 %) with a 10 % yield of CH_2OO; 40 % of the total

14   C9-CI are calculated to be stabilised at 1 atm. If all of the CH_2OO is assumed to be formed

15   stabilised (e.g. Nguyen et al., 2009) then this gives a total SCI yield of 46 %. Earlier

16   experimental studies have tended to determine lower total SCI yields with Hasson et al.

17   (2001) reporting a total SCI yield of 0.27 from measured product yields (almost entirely

18   nopinone) and Hatakeyama et al. (1984) reporting a total SCI yield of 0.25. Winterhalter et al.

19   (2000) determined a yield of 0.16 (± 0.04) for excited CH_2OO from β-pinene ozonolysis,

20   obtained via the nopinone yield and 0.35 for the stabilised C9-CI, giving a total SCI yield of

21   0.51 of all the CH_2OO is assumed to be stabilised. Also, experimental studies have tended to

22   report higher CH_2OO yields (determined from measured nopinone yields) than theoretical

23   studies. Nguyen et al. (2009) note that this could be because nopinone can also be formed in

24   bimolecular reactions of SCI-4, hence experimental studies may overestimate CH_2OO

25   production. The MCMv3.3.1 incorporates a total SCI yield of 0.25 from β-pinene ozonolysis,

26   with a yield of stabilised C9-CI of 0.102 and a CH_2OO yield of 0.148.

27   ### 1.2.3 Limonene derived SCI

28   Limonene has two double bonds at which ozone can react. Theory suggests that reaction at

29   the endocyclic bond is more likely; Baptista et al. (2011) calculate reaction at the endo-cyclic

30   bond to be 84 – 94 % (dependent on the level of theory applied). Zhang et al. (2006) suggest

31   the reaction at the endo-cyclic double bond to be roughly 25 times faster than at the exo-

32   cyclic bond, i.e. leading to a branching ratio of ca. 96 % reaction at the endo bond and the

Atmospheric
Chemistry
and Physics
Discussions

1   current IUPAC recommendation (IUPAC, 2013) suggests about 95 % of the primary ozone

2   reaction to be at the endo bond. Leungsakul et al. (2005) reported a best fit to measurements

3   from chamber experiments by assuming an 85 % reaction at the endo-cyclic bond and 15 % at

4   the exo-cyclic bond.

5   Ozone reaction at the endo-cyclic bond of limonene produces four different C_{10} CI (Scheme

6   4: CI-5a, 5b, 6a, 6b). Similar to CI-1 and CI-2 from α-pinene, CI-5 is a mono-substituted CI

7   for which both *syn* (5a) and *anti* (5b) conformers exist, while the other, CI-6, is di-substituted,

8   for which two *syn*-conformers (6a and 6b) exist. Leungsakul et al. (2005) determined a total

9   SCI yield from limonene ozonolysis of 0.34, consisting of CH_2OO (0.05), CI-7 (0.04), CI-5

10 (0.15) and CI-6 (0.11). Sipilä et al. (2014) determined a total SCI yield of 0.27 (± 0.12) from

11 indirect experiments measuring the production of H_2SO_4 from SO_2 oxidation in the presence

12 of the limonene-ozone system. The MCMv3.3.1 describes only reaction with ozone at the

13 endocyclic double bond and recommends a total SCI yield of 0.135 with stabilisation of only

14 the mono-substituted CI-5.

15

16 **2   Experimental**

17 **2.1   Experimental Approach**

18 The EUPHORE facility is a 200 m^3 simulation chamber used primarily for studying reaction

19 mechanisms under atmospheric boundary layer conditions. Further details of the chamber

20 setup and instrumentation are available elsewhere (Becker, 1996; Alam et al., 2011), and a

21 detailed account of the experimental procedure, summarised below, is given in Newland et al

22 (2015a).

23 Experiments comprised time-resolved measurement of the removal of SO_2 in the presence of

24 the monoterpene-ozone system, as a function of humidity. SO_2 and O_3 abundance were

25 measured using conventional fluorescence and UV absorption monitors, respectively; alkene

26 abundance was determined via FTIR spectroscopy. Experiments were performed in the dark

27 (*i.e.* with the chamber housing closed; $j(NO_2) \leq 10^{-6}$ s^{-1}), at atmospheric pressure (*ca.* 1000

28 mbar) and temperatures between 287 and 302 K. The chamber is fitted with large horizontal

29 and vertical fans to ensure rapid mixing (*ca.* 2 minutes). Chamber dilution was monitored via

30 the first order decay of an aliquot of SF_6, added prior to each experiment. Cyclohexane (*ca.*

31 75 ppmv) was added at the beginning of each experiment to act as an OH scavenger, such that

1 SO$_2$ reaction with OH was calculated to be $\leq$ 1 % of the total chemical SO$_2$ removal in all

2 experiments.

3 Experimental procedure, starting with the chamber filled with clean scrubbed air, comprised

4 addition of SF$_6$ and cyclohexane, followed by water vapour, O$_3$ (*ca.* 500 ppbv) and SO$_2$ (*ca.*

5 50 ppbv). A gap of five minutes was left prior to addition of the monoterpene, to allow

6 complete mixing. The reaction was then initiated by addition of the monoterpene (*ca.* 400

7 ppbv for α-pinene and β-pinene, *ca.* 200 ppbv for limonene), and reagent concentrations

8 followed for roughly 30 - 60 minutes; *ca.* 30 – 90 % of the monoterpene was consumed after

9 this time, dependent on the reaction rate with ozone. Four α-pinene + O$_3$, five β-pinene + O$_3$,

10 and five limonene + O$_3$ experiments, as a function of [H$_2$O], were performed in total. Each

11 individual run was performed at a constant humidity, with humidity varied to cover the range

12 of [H$_2$O] = 0.1 – 19 × 10^{16} molecules cm^{-3}, corresponding to an RH range of 0.1 – 28 % (at

13 298 K). Measured increases in [SO$_2$] agreed with measured volumetric additions across the

14 SO$_2$ and humidity ranges used in the experiments (Newland et al., 2015a).

15 **2.2 Analysis**

16 A range of different SCI are produced from the ozonolysis of each of the three monoterpenes

17 (see Schemes 2 – 4), each with their own distinct chemical behaviour (*i.e.* yields, reaction

18 rates); it is therefore not feasible (from these experiments) to obtain data for each SCI

19 independently; consequently, for analytical purposes we necessarily treat the SCI population

20 in a simplified (lumped) manner – see Section 2.2.2.

21 SCI are assumed to be formed in the ozonolysis reaction with a yield φ (Reaction R1). They

22 can then react with SO$_2$, with H$_2$O, with acids formed in the ozonolysis reaction, with other

23 species present, or undergo unimolecular decomposition, under the experimental conditions

24 applied (Reactions R2 – R5). A fraction of the SCI produced reacts with SO$_2$. This fraction (*f*)

25 is the loss rate of the SCI to SO$_2$ (k_2[SO$_2$]) compared to the sum of the total loss processes for

26 the SCI (Equation E1) :

27
$$f = \frac{k_2[\text{SO}_2]}{k_2[\text{SO}_2] + k_3[\text{H}_2\text{O}] + k_d + k_5[\text{acid}] + \text{L}} \qquad (E1)$$

28 Here, *L* accounts for the sum of any other chemical loss processes for SCI in the chamber,

29 with the exception of reaction with acids these loss processes are expected to be negligible, as

1   discussed later. After correction for dilution, and neglecting other (non-alkene) chemical sinks

2   for O_3, such as reaction with HO_2 (also produced directly during alkene ozonolysis (Alam et

3   al., 2013; Malkin et al., 2010)), which was indicated through model calculations to account

4   for < 0.5 % of ozone loss under all the experimental conditions, the following equation is

5   derived:

$$\frac{dSO_2}{dO_3} = \phi.f$$

6   (E2)

7   From Equation E2, regression of the loss of ozone (dO_3) against the loss of SO_2 (dSO_2) for an

8   experiment at a given RH determines the product $f.\phi$ at a given point in time. This quantity

9   will vary through the experiment as SO_2 is consumed, and other potential SCI co-reactants are

10   produced, as predicted by Equation E1. A smoothed fit was applied to the experimental data

11   for the cumulative consumption of SO_2 and O_3, ΔSO_2 and ΔO_3, (as shown in Figure 2) to

12   determine dSO_2/dO_3 (and hence $f.\phi$) at the start of each experiment, for use in Equation E2.

13   The start of each experiment (*i.e.* when $[SO_2] \sim 50$ ppbv) was used as this corresponds to the

14   greatest rate of production of the SCI, and hence largest experimental signals (*i.e.* greatest O_3

15   and SO_2 rate of change; greatest precision) and is the point at which the SCI + SO_2 reaction

16   has the greatest magnitude compared with any other potential loss processes for either

17   reactant species (see discussion below).

18   Other potential fates for SCIs include reaction with ozone (Kjaergaard et al., 2013; Vereecken

19   et al., 2014; Wei et al., 2014; Vereecken et al., 2015), with other SCI (Su et al., 2014;

20   Vereecken et al., 2014), carbonyl products (Taatjes et al., 2012), acids (Welz et al., 2014), or

21   with the parent alkene (Vereecken et al., 2014; Decker et al., 2017). Sensitivity analyses using

22   the most recent theoretical predictions (Vereecken et al., 2015) indicate that the reaction with

23   ozone may be significant under certain conditions, accounting for up to 7% of SCI loss for

24   *anti*-SCI (based on *anti*-CH_3CHOO) at the lowest RH (worst case) experiment. However,

25   generally SCI loss to ozone is calculated to be < 5% for *anti*-SCI and < 1% for *syn*-SCI.

26   Summed losses from reaction with SCI (self-reaction), carbonyls and alkenes are calculated to

27   account for < 1 % of the total SCI loss under the experimental conditions applied.

28   CH_2OO and CH_3CHOO have been shown to react rapidly ($k = 1 - 5 \times 10^{-10}$ cm^3 s^{-1}) with

29   formic and acetic acid (Welz et al., 2014). In ozonolysis experiments, Sipilä et al. (2014)

30   determined the relative reaction rate of acetic and formic acids with $(CH_3)_2COO$ (i.e. k_5/k_2)

31   be roughly three. Organic acid mixing ratios in this work, as measured by FTIR, reached up to

1   a few hundreds of ppbv, suggesting these will likely be a significant SCI sink in our

2   experiments. We have therefore explicitly included reaction with organic acids in our

3   analysis, incorporating the uncertainty arising from the (unknown) acid reaction rate constant,

4   as described in Section 2.2.1.

5   To date, the effects of the water dimer, $(H_2O)_2$ on SCI removal have only been determined

6   experimentally for CH_2OO (Berndt et al., 2014; Chao et al., 2015; Lewis et al., 2015;

7   Newland et al., 2015a). Theoretical calculations (Vereecken and Francisco, 2012) predicted

8   the significant effect of the water dimer compared to the monomer for CH_2OO, but also that

9   the ratio of the SCI + $(H_2O)_2$: SCI + H_2O rate constants, k_5/k_3, of the larger, more substituted

10 SCI, *anti*-CH_3CHOO and $(CH_3)_2COO$, are 2 - 3 orders of magnitude smaller than for CH_2OO

11 (Vereecken and Francisco, 2012). This would make the dimer reaction negligible at

12 atmospherically accessible $[H_2O]$ (*i.e.* $< 1 \times 10^{18} \, cm^{-3}$) for SCI larger than CH_2OO. Therefore,

13 the effect of the water dimer reaction with C_{10}– and C_9–SCI is not considered in this analysis.

14 For CH_2OO, the reaction rates with water and the water dimer have been quantified in recent

15 EUPHORE experimental studies, and the values from Newland et al. (2015a) are used.

2.2.1 Derivation of $k(SCI+H_2O)/k(SCI+SO_2)$ and $k_d/k(SCI+SO_2)$

17 As noted above, a range of different SCI are produced from the ozonolysis of the three

18 monoterpenes (see Schemes 2 – 4), each with their own distinct chemical behaviour, which

19 treated individually, introduce too many unknowns (*i.e.* yields, reaction rates) for explicit

20 analysis. Consequently for analytical purposes we treat the SCI population in a simplified

21 (lumped) manner:

22 Firstly, we use the simplest model possible, assuming that a single SCI is formed in each

23 ozonolysis reaction (Equation E3).

$$\frac{f}{[SO_2]} = \left([SO_2] + \frac{k_3}{k_2}[H_2O] + \frac{k_d}{k_2} + \frac{k_5}{k_2}[acid] \right)^{-1} \quad (E3)$$

25 Secondly, for each monoterpene, the SCI produced are assumed to belong to one of two

26 populations, denoted SCI-A and SCI-B. These two populations are split according to the

27 observation that the decomposition rates and reaction rates with water for the smaller SCI

28 (CH_3CHOO) have been predicted theoretically (Ryzhkov and Ariya, 2004; Kuwata et al.,

29 2010; Anglada et al., 2011) and shown experimentally (Taatjes et al., 2013; Sheps et al.,

1   2014; Newland et al., 2015a) to exhibit a strong dependence on the structure of the molecule.

2   The syn-CH_3CHOO conformer, which has the terminal oxygen of the carbonyl oxide moiety

3   in the syn position to the methyl group, has been shown to react very slowly with water and to

4   readily decompose, via the hydroperoxide mechanism; whereas the $anti$-CH_3CHOO

5   conformer, with the terminal oxygen of the carbonyl oxide moiety in the $anti$-position to the

6   methyl group, has been shown to react fast with water and is not able to decompose via the

7   hydroperoxide mechanism. Vereecken and Francisco (2012) have shown that all SCI studied

8   theoretically with an alkyl group in the syn position have reaction rates with H_2O of $k < 4 \times$

9   10^{-17} molecule cm^3 s^{-1} (and for SCI larger than acetone oxide, $k < 8 \times 10^{-18}$ molecule cm^3 s^{-1}).

10   We thus define two populations, assuming SCI-A (i.e. SCI that exhibit chemical properties of

11   the $anti$-type SCI) to react fast with water and not to undergo unimolecular reactions, and

12   SCI-B (i.e. SCI that exhibit chemical properties of the syn type SCI) to not react with water

13   but to undergo unimolecular reactions. This simplification allows us to fit to the

14   measurements using Equations E4 and E5, as shown below. The total SCI yields are

15   determined by our experiments at high SO_2, and the relative yields of SCI-A and SCI-B are

16   determined from fitting to Equation E5. These relative yields are then compared to those

17   predicted from the literature.

18   In this model, $f = \gamma^A f^A + \gamma^B f^B$, where γ is the fraction of the total SCI yield (i.e. $\gamma^A + \gamma^B = 1$). f^A

19   and f^B are the fractional losses of SCI-A and SCI-B to reaction with SO_2. Adapting Equation

20   E1 to include the two SCI species gives Equation E4, where $k_5[acid]$ accounts for the SCI +

21   acid reaction (see discussion of reaction rate constants below).

22   $$f = \frac{\gamma^A k_2^A [SO_2]}{k_2^A [SO_2] + k_3 [H_2O] + k_5^A [acid]} + \frac{\gamma^B k_2^B [SO_2]}{k_2^B [SO_2] + k_d + k_5^B [acid]} \qquad (E4)$$

23   Equation E4 can be rearranged to Equation E5 and fitted according to $f/[SO_2]$ derived from

24   the measurements.

25   $$\frac{f}{[SO_2]} = \frac{\gamma^A}{[SO_2] + \frac{k_3}{k_2^A}[H_2O] + \frac{k_5^A}{k_2^A}[acid]} + \frac{\gamma^B}{[SO_2] + \frac{k_d}{k_2^B} + \frac{k_5^B}{k_2^B}[acid]} \qquad (E5)$$

26   Using values for γ^A and γ^B from the literature and varying the assumed values of the reaction

27   of SCI with acid (k_5) allows us to determine k_3/k_2^A and k_d/k_2^B.

Atmospheric
Chemistry
and Physics
Discussions

1   The assumptions made here allow analysis of a very complex system. However, a key

2   consequence is that the relative rate constants obtained from the analysis presented here are

3   not representative of the elementary reactions of any single specific SCI isomer formed, but

4   rather represent a quantitative ensemble description of the integrated system, under

5   atmospheric boundary layer conditions, which may be appropriate for atmospheric modelling.

6   Additionally our experimental approach cannot determine absolute rate constants (*i.e.* values

7   of k_2, k_3, k_d) in isolation, but is limited to assessing their relative values, measured under

8   atmospheric conditions, which may be placed on an absolute basis through use of an external

9   reference value (here the SCI + SO_2 rate constant).

2.2.2   SCI yield calculation

11 The value for the total SCI yield of each monoterpene, $\phi_{SCI-TOT}$, was determined from an

12 experiment performed under dry conditions (RH < 1%) in the presence of excess SO_2 (*ca.*

13 1000 ppbv), such that SO_2 scavenged the majority of the SCI. From Equation E2, regressing

14 dSO_2 against dO_3 (corrected for chamber dilution), assuming f to be unity (*i.e.* all the SCI

15 produced reacts with SO_2), determines the value of ϕ_{min}, a lower limit to the SCI yield. Figure

16 1 shows the experimental data, from which ϕ_{min} was derived.

17 In reality f will be less than one, at experimentally accessible SO_2 levels, as a fraction of the

18 SCI may still react with trace H_2O present, or undergo unimolecular reaction. The actual

19 yield, ϕ_{SCI}, was determined by combining the result from the excess-SO_2 experiment with

20 those from the series of experiments performed at lower SO_2, as a function of $[H_2O]$, to obtain

21 k_3/k_2 and k_d/k_2 (see Section 2.2.1), through an iterative process to determine the single unique

22 value of ϕ_{SCI} which fits both datasets, as described in Newland et al. (2015a), but taking into

23 account the proposed model in this paper of there being two SCI produced. In this model, $f =$

24 $\gamma^A f^A + \gamma^B f^B$. Where $f^A = [SO_2] / ([SO_2] + k_3[H_2O]/k_2)$ and $f^B = [SO_2] / ([SO_2] + k_d/k_2)$ – other

25 possible SCI sinks are assumed to be negligible. In these excess-SO_2 experiments, $f^A \sim 1$ but

26 $f_B < 1$ since k_d still represents a significant sink.

27 γ^A (and hence γ^B, since $\gamma^B = 1 - \gamma^A$) is derived from fitting Equation E4 to the data from the

28 experiments performed at lower SO_2 for a given ϕ. Using a range of ϕ, gives a range of γ.

29 These different values of γ are used with the respective values of ϕ in fitting to Equation E4

30 to determine values of k_3/k_2 and k_d/k_2.

31

3   Theoretical calculations

2   The rovibrational characteristics of all conformers of the CI formed from α-pinene and β-

3   pinene, the transition states for their unimolecular reaction, and for their reaction with H_2O,

4   were characterized quantum chemically, first using the M06-2X/cc-pVDZ level of theory, and

5   subsequently refined at the M06-2X/aug-cc-pVTZ level. To obtain accurate barrier heights for

6   reaction, it has been shown (Berndt et al., 2015; Chhantyal-Pun et al., 2017; Fang et al.,

7   2016a, 2016b; Long et al., 2016; Nguyen et al., 2015) that post-CCSD(T) calculations are

8   necessary. Unfortunately, performing such calculations for the SCI discussed in this paper,

9   with up to 14 non-hydrogen atoms, is well outside our computational resources, though

10 CCSD(T)/aug-cc-pVTZ single point energy calculations were performed for the unimolecular

11 reactions of nopinone oxides and the most relevant subset of pinonaldehyde oxides. These

12 data are sufficient for relative rate estimates, but it remains useful to improve the absolute

13 barrier height predictions, using the data set by Vereecken et al. (Vereecken et al., 2017). This

14 data set has a large number of systematic calculations on smaller CI, allowing empirical

15 corrections to the DFT or CCSD(T) barrier heights to estimate the post-CCSD(T) barrier

16 heights. The methodology for these corrections is described in more detail in Vereecken et al.

17 (2017); briefly, it compares rate coefficient calculations against available harmonized

18 experimental and very-high level theoretical kinetic rate predictions, and adjusts the barrier

19 heights by 0.4 to 2.6 kcal mol^{-1} (depending on the base methodology and the reaction type) to

20 obtain best agreement with these benchmark results.

21 Using the energetic and rovibrational data thus obtained, multi-conformer transition state

22 theory (MC-TST) calculations (Truhlar et al., 1996; Vereecken and Peeters, 2003) were

23 performed to obtain the rate coefficient at 298K at the high pressure limit. All rate predictions

24 incorporate tunnelling corrections using an asymmetric Eckart barrier (Eckart, 1930; Johnston

25 and Heicklen, 1962). For the reaction of CI + H_2O, a pre-reactive complex is postulated at 7

26 kcal mol^{-1} below the free reactants, while the CI + $(H_2O)_2$ reaction is taken to have a pre-

27 reactive complex of 11 kcal mol^{-1} stability. This pre-reactive complex affects tunnelling

28 corrections; it is assumed that this pre-reactive complex is always in equilibrium with the free

29 reactants.

30 In view of the high number of rotamers and the resulting computational cost, only a single

31 limonene-derived CI isomer was studied, where the TS for the CI + H_2O reaction was

32 analyzed at the M06-2X/cc-pVDZ level of theory with only a partial conformational analysis;

1   a limited number of the energetically most stable TS conformers thus discovered were re-

2   optimized at the M06-2X/aug-cc-pVTZ level of theory. These data will only be used for

3   qualitative assessments. However, we apply the structure-activity relationships (SARs)

4   presented by Vereecken et al. (Vereecken et al., 2017) to obtain an estimate of the rate

5   coefficients, and assess the role of the individual SCI isomers in limonene ozonolysis.

6   All quantum chemical calculations were performed using Gaussian-09 (Frisch et al., 2010).

7

8   4   GEOS-Chem Model Simulation

9   The global chemical transport model GEOS-Chem (v9-02, www.geos-chem.org, Bey et al.,

10   2002) is used to explore the spatial and temporal variability of the atmospheric impacts of the

11   experimentally derived chemistry. The model includes HOx-NOx-VOC-O_3-BrOx chemistry

12   (Mao et al., 2010; Parrella et al., 2012) and a mass-based aerosol scheme. Biogenic

13   monoterpene emissions are taken from the Model of Emissions of Gases and Aerosols from

14   Nature (MEGAN) v2.1 inventory (Guenther et al., 2006; 2012). Transport is driven by

15   assimilated meteorology (GEOS-5) from NASA's Global Modelling and Assimilation Office

16   (GMAO). The model is run at 4°×5° resolution, with the second year (2005) used for analysis

17   and first year discarded as spin up.

18   In this study, the standard simulation was expanded to include emissions of seven

19   monoterpene species (α-pinene, β-pinene, limonene, myrcene, ocimene, carene, and sabinene)

20   from MEGAN v2.1. The ozonolysis scheme for each monoterpene, detailed in Section 6.1,

21   considers the formation of one or two types of SCI, and their subsequent reaction with SO_2,

22   H_2O, or unimolecular decomposition. Reaction rate of the monoterpenes with OH, O_3 and

23   NO_3 rare detailed in Table S1.

24

25   5   Results

26   5.1   SCI Yield

27   Figure 1 shows the lower limit to the SCI yield, ϕ_{min}, for the three monoterpenes, determined

28   from fitting Equation E5 to the experimental data. This gives values of 0.16 (± 0.01) for α-

29   pinene, 0.53 (± 0.01) for β-pinene and 0.20 (± 0.01) for limonene. These ϕ_{min} values were

30   then corrected as described in Section 2.2.2 using the k_3/k_2 and k_d/k_2 values determined from

Atmospheric
Chemistry
and Physics
Discussions

1   the measurements shown in Figures 3 − 5 using Equation E4. The corrected yields, ϕ_{SCI}, are

2   0.19 ($\pm$ 0.01) for α-pinene, 0.60 ($\pm$ 0.03) for β-pinene and 0.23 ($\pm$ 0.01) for limonene.

3   Uncertainties are $\pm$ 2σ, and represent the combined systematic (estimated measurement

4   uncertainty) and precision components. Literature yields for SCI production from

5   monoterpene ozonolysis are summarised in Table 1.

6   The value derived for the total SCI yield from α-pinene in this work of 0.19 agrees, within the

7   uncertainties, with the value of 0.15 ($\pm$ 0.07) reported by Sipilä et al. (2014) and the value of

8   0.20 applied in the MCMv3.3.1.

9   The total SCI yield from β-pinene derived in this work, 0.60, agrees reasonably well with the

10 recent experimental work of Ahrens et al. (2014) who derived a total SCI yield of 0.50 (0.40

11 for the sum of CI-1 and CI-2 and 0.10 for CH_2OO, which is assumed to be formed almost

12 completely stabilised). The MCMv3.3.1 applies a total SCI yield of 0.25, of which 0.10 is a

13 C9-CI and 0.15 is CH_2OO. Earlier studies also tended to derive lower total SCI yields ranging

14 from 0.25 – 0.27 (Hasson et al., 2001; Hatakeyama et al., 1984).

15 The total SCI yield from limonene derived in this work, 0.23 ($\pm$ 0.01) agrees with the recently

16 determined yield from Sipilä et al. (2014) of 0.27 ($\pm$ 0.12). Leungsakul et al. (2005) derived a

17 somewhat higher yield of 0.34, while the MCMv3.3.1 applies a lower yield of 0.135.

18 **5.2 $k_3(SCI+H_2O)/k_2(SCI+SO_2)$ and $k_d/k_2(SCI+SO_2)$ Analysis**

19 Figure 2 shows the loss of SO_2 as ozone is consumed by reaction with the monoterpene for

20 each of the three systems. Box modelling results suggest that > 99 % of this SO_2 removal is

21 caused by reaction with SCI produced in the alkene-ozone reaction (rather than e.g. reaction

22 with OH, which is scavenged by cyclohexane). When the experiments are repeated at higher

23 relative humidity, the rate of loss of SO_2 decreases. This is as expected from Equation E1 and

24 suggests that there is competition between SO_2 and H_2O for reaction with the SCI produced,

25 in agreement with observations of smaller SCI, which demonstrate the same competition

26 under atmospherically relevant conditions (Newland et al., 2015a; Newland et al., 2015b).

27 However, as the relative humidity is increased further, the SO_2 loss does not fall to (near) zero

28 as would be expected from Equation E1. This suggests that at high [H_2O] the amount of SO_2

29 loss becomes less sensitive to [H_2O]. This is most likely due to there being at least two

30 chemically distinct SCI species present. This behaviour was previously observed for

1   CH$_3$CHOO by Newland et al. (2015a) and fits with the current understanding that the

2   reactivity of SCI is structure dependent.

3   To recap Section 2.2.1, the analysis presented here considers two models to fit the

4   observations. The first of these (Equation E3) assumes the formation of a single SCI species,

5   which, in addition to reacting with SO$_2$, can react with water, undergo unimolecular reaction

6   or react with acid. It is clearly evident from Figures 3 – 5 that this model does not give a good

7   fit to the observations for any of the monoterpene systems studied. Therefore, the results from

8   this (single SCI) approach are not discussed explicitly hereafter. The second of the models

9   (Equation E5) assumes the formation of two lumped, chemically distinct, populations of SCI,

10 denoted SCI-A and SCI-B. SCI-A is assumed to react fast with H$_2$O and to have minimal

11 decomposition. Conversely, SCI-B is assumed to have a negligible reaction with water under

12 the experimental conditions applied but to undergo rearrangement via a VHP. We use a least-

13 squares fit of Equation E5 to the data to determine the values of k_3/k_2 and k_d/k_2. This approach

14 fits the data well (Figures 3 - 5) for all 3 monoterpenes and represents the overall attributes of

15 the SCI formed - but as noted, does not represent an explicit determination of individual

16 conformer-dependent rate constants.

17 ### 5.2.1 α-pinene

18 The α-pinene system is sensitive to water vapour at the low H$_2$O range, with the SO$_2$ loss

19 falling dramatically when the RH is increased from 0.1 to 2.5 % (Figure 2). However, at

20 higher RH the SO$_2$ loss appears to be rather insensitive to [H$_2$O].

21 CI-1 can be formed in either *syn* (1a) or *anti* (1b) configuration, whereas both CI-2

22 conformers formed are in a *syn* configuration (see Scheme 2). For one of the two conformers

23 of CI-2 (CI-2b), the hydrogen atom available for abstraction by the terminal oxygen of the

24 carbonyl oxide group is attached to the carbon on the four-membered ring. This has been

25 shown in the β-pinene system to make a large difference with respect to the ability of the

26 hydrogen to be abstracted and to undergo the VHP mechanism (Rickard et al., 1999; Nguyen

27 et al., 2009). This therefore suggests that CI-2b may exhibit characteristics of both SCI-A and

28 SCI-B. Ma et al. (2008) infer a probable equal yield of the two basic CI structures. This

29 would suggest a relative yield for SCI-A of 0.25 – 0.50 (depending on the precise nature of

30 CI-2b). Fitting Equation E4 to the data and allowing lambda to vary determines values of $\gamma^A =$

31 0.40 and $\gamma^B = 0.60$ (Figure 3).

Atmospheric
Chemistry
and Physics
Discussions

1   In Figure 3, Equation E4 is fitted to the α-pinene measurements, assuming

2   $k(SCI+acid)/k(SCI+SO_2) = 0$. This derives a minimum value for $k(SCI-A+H_2O)/k(SCI-$

3   $A+SO_2)$, the water dependent fraction of the SCI, and a maximum value for

4   $k(decomposition:SCI-B)/k(SCI-B+SO_2)$, the water independent fraction of the SCI. The

5   kinetic parameters derived from the fitting are displayed in Table 2.

6   Figure 6 shows the variation of the derived k_3/k_2 and k_d/k_2 values as the ratio k_5/k_2,

7   $k(SCI+acid)/k(SCI+SO_2)$, is varied from zero to one. The derived k_3/k_2 increases by about 40

8   % from 1.4 (± 0.34) × 10^{-3} to 2.0 (± 0.49) × 10^{-3}. The derived k_d/k_2 value decreases, again by

9   about 40 %, from 8.2 (± 1.5) × 10^{12} cm^{-3} to 5.1 (± 0.93) × 10^{12} cm^{-3}.

10 The derived limits to the relative rate constants can be put on an absolute scale using the

11 $k(SCI+SO_2)$ values for CH$_3$CHOO from Sheps et al. (2014) for the *syn* and *anti* conformers.

12 These are, *syn*: 2.9 × 10^{-11} cm^3 s^{-1} and *anti*: 2.2 × 10^{-10} cm^3 s^{-1}. The *syn* rate constant is applied

13 to the derived $k(decomposition:SCI-B)/k(SCI-B+SO_2)$ value and the *anti* rate constant to the

14 $k(SCI-A+H_2O)/k(SCI-A+SO_2)$ value. It should be noted that the k_2 values are for quite

15 different SCI to those formed in this study and to our knowledge no structure specific

16 $k(SCI+SO_2)$ have been reported for monoterpene derived SCI, though Ahrens et al. (2014)

17 determine an average $k_2 \sim 4 \times 10^{-11}$ cm^3 s^{-1} for SCI derived from β-pinene, i.e. a value within

18 an order of magnitude of those determined for the smaller SCI CH$_2$OO, CH$_3$CHOO and

19 (CH$_3$)$_2$COO (e.g. Welz et al., 2012; Taatjes et al., 2013; Sheps et al., 2014; Huang et al.,

20 2015). Using the Sheps et al. (2014) values yields $k(SCI-A+H_2O) > 3.1$ (± 0.75) × 10^{-13} cm^3 s^{-}

21 ^{1} and $k(decomposition:SCI-B) < 240$ (± 44) s^{-1} (using the values derived for $k(SCI-$

22 $A+acid)/k(SCI-A+SO_2) = 0$). This k_3 value is an order of magnitude larger than the rate

23 constants determined for the smaller *anti*-CH$_3$CHOO in the direct studies of Sheps et al.

24 (2014) (2.4 × 10^{-14} cm^3 s^{-1}) and Taatjes et al. (2013) (1.0 × 10^{-14} cm^3 s^{-1}). The decomposition

25 value derived for SCI-B is of the same order of magnitude as that for *syn*-CH$_3$CHOO (348 ±

26 332 s^{-1}) and (CH$_3$)$_2$COO (819 ± 190 s^{-1}) from Newland et al., (2015a) (using updated direct

27 measurement values of k_2 from Sheps et al. (2014) and Huang et al. (2015) for *syn*-

28 CH$_3$CHOO and (CH$_3$)$_2$COO respectively) and within the range from the recent paper by

29 Smith et al. (2016) which derives a decomposition rate for (CH$_3$)$_2$COO of 269 (± 82) s^{-1} at

30 283 K increasing to 916 (± 56) s^{-1} at 323 K.

31 Sipilä et al. (2014) applied a single-SCI analysis approach to the formation of H$_2$SO$_4$ from

32 SO$_2$ oxidation in the presence of the α-pinene ozonolysis system. They determined that for α-

Atmospheric
Chemistry
and Physics
Discussions

1   pinene, $k_d \gg k(\text{SCI}+\text{H}_2\text{O})[\text{H}_2\text{O}]$ for $[\text{H}_2\text{O}] < 2.9 \times 10^{17}$ cm^{-3}, i.e. that the fate of SCI formed

2   in the system is rather insensitive to $[\text{H}_2\text{O}]$. Across the $[\text{SO}_2]$ and RH ranges used in their

3   study, the results obtained here would indicate H_2O to always be the dominant sink for SCI-

4   A, i.e. the fact that Sipilä et al. (2014) see similar H_2SO_4 production across the RH range in

5   their study is consistent with these results.

6

5.2.2 β-pinene

8   Two recent studies (Nguyen et al., 2009; Ahrens et al., 2014) have suggested yields of the two

9   C_9-CI (CI-3 and CI-4, see Scheme 3) obtained from β-pinene ozonolysis to be roughly equal.

10 In these studies Ahrens et al. (2014) assume a CH_2OO yield of 0.10 while Nguyen et al.

11 (2009) determine theoretically the yield of CH_2OO to be 0.05. Another theoretical study

12 (Zhang and Zhang, 2005) predicted a CH_2OO yield of 0.08. In experimental studies,

13 Winterhalter et al. (2000) determined the CH_2OO yield to be 0.16 (± 0.04) from measuring

14 the nopinone yield and assuming it to be entirely a primary ozonolysis product (i.e. the co-

15 product of CH_2OO formation) and Ma and Marston (2008) determine a summed contribution

16 of 84 % (± 0.03) for the two C_9-CI (i.e. a 16 % CH_2OO yield). The theoretical studies are

17 somewhat lower than the experimental but Nguyen et al. (2009) note that CI-4 is likely to

18 form additional nopinone in bimolecular reactions. The CH_2OO is assumed to all be formed

19 stabilised (e.g. Nguyen et al. 2009).

20 SCI-3 is expected to undergo unimolecular reactions at least an order of magnitude faster than

21 SCI-4 (Nguyen et al., 2009; Ahrens et al., 2014). The reaction of SCI-3 with water is expected

22 to be slow based on the calculations presented in Table 4, with a pseudo first order reaction

23 rate of 1.0 s^{-1} at 75 % RH, 298 K, whereas the water reaction with SCI-4 is expected to be

24 considerably faster with a pseudo first order reaction rate of 240 s^{-1} at 75 % RH, 298 K. This

25 reaction will thus likely be the dominant fate of SCI-4 at typical atmospheric RH. This is in

26 agreement with the observations of Ma and Marston (2008), that show a clear dependence of

27 nopinone formation on RH (presumed to be formed from SCI + H_2O). Fitting Equation E4 to

28 the data determines values of $\gamma^A = 0.41$ and $\gamma^B = 0.59$ (Figure 4).

29 Using these values, and assuming $k(\text{SCI}+\text{acid})/k(\text{SCI}+\text{SO}_2) = 0$, yields a $k(\text{SCI-}$

30 $\text{A}+\text{H}_2\text{O})/k(\text{SCI-A}+\text{SO}_2)$ value of > 1.0 (± 0.27) $\times 10^{-4}$ and a $k(\text{decomposition:SCI-B})/k(\text{SCI-}$

31 $\text{B}+\text{SO}_2)$ value of < 6.0 (± 1.3) $\times 10^{12}$ cm^{-3} (Table 2).

1   As shown in Figure 6, increasing k_5/k_2, $k(SCI+acid)/k(SCI+SO_2)$, from zero to one, decreases

2   the derived k_d/k_2 from 6.0 ($\pm$ 1.3) $\times 10^{12}$ cm^{-3} to 1.8 ($\pm$ 0.39) $\times 10^{12}$ cm^{-3}. The derived k_3/k_2

3   increases by a factor of four from 1.0 ($\pm$ 0.27) $\times 10^{-4}$ to 3.7 ($\pm$ 1.0) $\times 10^{-4}$.

4   These values can be put on an absolute scale (using the values derived above for $k_5/k_2 = 0$).

5   For SCI-A, $k(SCI+SO_2)$ is taken as the experimentally determined value of 4×10^{-11} cm^3 s^{-1}

6   from Ahrens et al. (2014). For SCI-B, the syn-CH$_3$CHOO $k(SCI+SO_2)$ value determined by

7   Sheps et al. (2014) is used. This gives values of $k(SCI\text{-}A+H_2O) > 4 \times 10^{-15}$ ($\pm$ 1) cm^3 s^{-1} and

8     $k(decomposition:SCI\text{-}B) < 170$ ($\pm$ 38) s^{-1}.

9   ### 5.2.3 Limonene

10   For the limonene measurements presented in Figure 2, $(dSO_2/dO_3)/dt$ appears to be non-

11   linear, with a jump in dSO_2/dO_3 between 120 and 150 ppbv of ozone consumed. This is most

12   evident in the two lowest RH runs (0.2 and 2.0 %). Limonene is the fastest reacting of the

13   systems presented here, with the alkene reaction having consumed 100 ppbv of ozone within

14   the first five minutes. The limonene sample required about five minutes of heating before the

15   entire sample was volatized and injected into the chamber. This therefore may account for the

16   apparent non-linear nature of dSO_2/dO_3 in Figure 2.

17   The SO$_2$ loss in the limonene-ozone system is less affected by increasing H$_2$O than for either

18   α or β-pinene (Figure 5), with the values of $f/[SO_2]$ (y-axis) varying by roughly a factor of two

19   over the RH range applied compared to more than a factor of three variation for the other two

20   systems. Hence it might be expected that there is little formation of H$_2$O dependent SCI or

21   that it has a rather slow reaction rate with water.

22   Fitting Equation E4 to the data determines values of $\gamma^A = 0.22$ and $\gamma^B = 0.78$ (Figure 5). This

23   is broadly in line with the ratio recommended in the MCMv3.3.1 of 0.27:0.73, and with that

24   proposed in Leungsakul et al. (2005) who use a CI-A:CI-B ratio of 0.35:0.65, but also include

25   some stabilisation of CH$_2$OO and C$_9$-CI from ozone reaction at the exo-cyclic bond. This

26   yields a $k(SCI\text{-}A+H_2O)/k(SCI\text{-}A+SO_2)$ value of < 3.5 ($\pm$ 0.20) $\times 10^{-5}$ and a

27     $k(decomposition:SCI\text{-}B)/k(SCI\text{-}B+SO_2)$ value of > 4.5 ($\pm$ 0.10) $\times 10^{12}$ cm^{-3}.

28   Figure 6 shows that the derived k_d/k_2 increases by about 7 % as $k(SCI+acid)/k(SCI+SO_2)$

29   ranges from 0.0 to 0.8. The derived k_3/k_2 becomes negative at $k(SCI+acid)/k(SCI+SO_2) > 0.8$,

30   putting an upper limit on this ratio, i.e. $k_5/k_2 < 0.8$, for the limonene system.

1   Putting these values on an absolute scale (using the values derived for $k_5/k_2 = 0$), using the

2   CH$_3$CHOO *syn* and *anti* k(SCI+SO$_2$) determined by Sheps et al. (2014), yields values of < 7.7

3   (± 0.60) × 10^{-15} cm^3 s^{-1} and > 130 (± 3) s^{-1} for k_3 and k_d respectively. These values are similar

4   to those derived for the SCI-A and SCI-B formed from β-pinene. The k_3 value is a factor of

5   three smaller than that determined by Sheps et al. (2014) for k_3(*anti*-CH$_3$CHOO+H$_2$O), 2.4 ×

6   10^{-14} cm^3 s^{-1}.

7   Sipilä et al. (2014) applied a single-SCI analysis approach to the formation of H$_2$SO$_4$ from

8   SO$_2$ oxidation by the limonene ozonolysis system and determined that, similarly to α-pinene,

9   k(decomp.) >> k(SCI+ H$_2$O)[H$_2$O] for [H$_2$O] < 2.9 × 10^{17} cm^{-3}, i.e. that the system is rather

10 insensitive to [H$_2$O]. Our data are consistent with the limonene system being less sensitive to

11 [H$_2$O] than the SCI populations derived from the other two monoterpenes reported here.

5.2.4 Experimental Summary

13 The removal of SO$_2$ in the presence of ozonolysis reactions of α-pinene, β-pinene and

14 limonene has been studied as a function of water vapour concentration, and analysed

15 following the approximation that the SCI population can be represented through a two species

16 model, with contrasting unimolecular decomposition rates and reactivity to water. The results

17 presented in this work suggest that all three monoterpenes studied produce a range of SCI that

18 have differing reactivities towards water and decomposition. This is in agreement with current

19 theoretical understanding but is the first experimental demonstration for large SCI derived

20 from monoterpene ozonolysis. The complex reactivity of the systems investigated is further

21 highlighted by the fact that the experimental data are not fitted well by the assumption of the

22 formation of a single SCI species. While the behaviour of large SCI derived from

23 monoterpenes are likely to be significantly more complicated than is accounted for by simply

24 considering the differing kinetics of *syn* and *anti* SCI conformers, this approach provides a

25 reasonable description of the experimental behaviour observed, and the results presented here

26 are broadly in line with experimental results from the smaller SCI and from theoretical

27 results. The reaction rates of SCI-A (i.e. SCI that exhibit chemical properties of the *anti*-type

28 SCI) derived from the three different monoterpenes with water range from < 0.8 to > 31 × 10^{-}

29 ^{14} cm^3 s^{-1}, broadly in line with the derived rates of Sheps et al. (2014) for *anti*-CH$_3$CHOO of

30 2.4 × 10^{-14} cm^3 s^{-1}. The decomposition rates of SCI-B (i.e. SCI that exhibit chemical

31 properties of the *syn*-type SCI) are on the order of 100 - 250 s^{-1}. This is in line with those

32 derived for *syn*-CH$_3$CHOO from *cis* and *trans*-but-2-ene ozonolysis and (CH$_3$)$_2$COO by

Atmospheric
Chemistry
and Physics
Discussions

Open Access

EGU

1   Newland et al. (2015a) of 348 (± 332) s^{-1} and 819 (± 190) s^{-1} respectively (assuming k(syn-

2   CH$_3$CHOO+SO$_2$) = 2.9 × 10^{-11} cm^3 s^{-1} (Sheps et al., 2014) and k((CH$_3$)$_2$COO+SO$_2$) = 2.9 ×

3   10^{-10} cm^3 s^{-1} (Huang et al., 2015)) and recent results from Smith et al. (2016) of 269 – 916 s^{-1}

4   (strongly dependent on temperature) for (CH$_3$)$_2$COO decomposition. In this work we only

5   derive relative rates, but the similarity of the k_3 and k_d values derived when the k_2 values for

6   syn and $anti$-CH$_3$CHOO from Sheps et al. (2014) are applied is consistent with the recent

7   work of Ahrens et al. (2014), suggesting that large SCI, derived from monoterpenes,

8   demonstrate a similar reactivity towards SO$_2$ as smaller SCI. One uncertainty in the derivation

9   of the kinetics presented herein is the reactions of the SCI produced with organic acids. These

10   acids were present in the experiments (owing to formation in the monoterpene ozonolysis

11   reactions themselves) at levels which may have been a competitive sink for the SCI.

12   The ability of the simplified SCI-A / SCI-B approach to fit the experimental data and the

13   good agreement with theory and experimental work for smaller SCI suggests that the kinetic

14   parameters derived herein, using a lumped two-SCI system, may be useful for modelling and

15   provide the best available basis for modelling the effects of SCI on atmospheric SO$_2$

16   oxidation in the presence of water vapour. To this end, in Section 6 we present the results of a

17   global modelling study using the kinetic parameters derived herein.

18   **5.3   Theoretical results and comparison to experiments**

19   The theoretically predicted rate coefficients for unimolecular reactions of the monoterpene

20   SCI are listed in Table 3, while those for the reaction with H$_2$O are listed in Table 4. These

21   data can be compared against the experimental data obtained in this work.

22   5.3.1 α-pinene

23   The theory-based rate coefficients show one pinonaldehyde oxide, CI-1b, with a rate of

24   reaction with water that is significantly faster than the remaining α-pinene-derived CI.

25   Comparing this rate to the experimental data suggests that CI-1b corresponds to SCI-A, with

26   matching rate coefficients within an order of magnitude, i.e. within the expected uncertainty.

27   We thus deduce that SCI-A is CI-1b. The remaining pinonaldehyde oxides, CI-1a, CI-2a and

28   CI-2b, react predominantly through unimolecular reactions, where theory-based rate

29   coefficients range from 60 to 600 s^{-1}, all within a factor of 4 of the experimentally derived

30   population-averaged rate of 240 ± 44 s^{-1}, i.e. matching within the uncertainty margins. The

1   unimolecular rate coefficients of this set of CI are sufficiently close that it is not feasible to

2   separate these in the experimental data, so we can only conclude that SCI-B in the α-pinene

3   ozonolysis experiments may consist of a mixture of C-1a, CI-2a and CI-2b.

5.3.2 β-pinene

5   The theoretical analysis for nopinone oxides shows one isomer, SCI-4, that has a fast rate of

6   reaction with water, but a slow unimolecular isomerisation, while the other isomer, SCI-3,

7   shows a fast unimolecular decomposition. These can thus be unequivocally equated to the

8   experimentally obtained SCI-A and SCI-B, respectively, inasmuch as the yield of CH_2OO is

9   minor. The predicted rate coefficients are within the expected uncertainty intervals of the

10   theoretical data, a factor of 5 for the unimolecular rates, and an order of magnitude for the

11   reaction with H_2O.

12   The experimental rate measurements are defined relative to the reaction rate with SO_2; the

13   value adopted for the $k(SCI+SO_2)$ reaction therefore influences the derived rate coefficient

14   values. Ahrens et al. (2014) directly measured the SO_2 rate coefficient of the longest-lived

15   SCI (SCI-4) to be $\sim 4 \times 10^{-11}$ cm^3 s^{-1}, but for SCI-3 we assume a similar rate coefficient as

16   syn-CH_3CHOO + SO_2 determined by Sheps et al. (2014) of 2.9×10^{-11} cm^3 s^{-1}. Nopinone

17   oxides are bicyclic compounds, with a bulky dimethyl-substituted 4-membered ring adjacent

18   to the carbonyl oxide moiety. To examine the potential impact of steric hindrance on the SCI

19   + SO_2 reaction, we characterized all sulfur-substituted secondary ozonides (S-SOZ) formed in

20   this reaction (Kuwata et al., 2015; Vereecken et al., 2012). We find that the tri-cyclic S-SOZ

21   shows very little interaction between the sulfur-bearing ring and the β-pinene substituents,

22   and little change in ring strain. The energies of the S-SOZ adducts relative to the SCI + SO_2

23   reactants thus remains very similar to that of CH_2OO, CH_3CHOO or $(CH_3)_2COO$, confirming

24   the quality of our selection of reference rate coefficients.

5.3.3 Limonene

26   Of the six non-CH_2OO CI formed in limonene ozonolysis, CI-5b was predicted to have a fast

27   reaction rate with H_2O; its oxide substitution patterns is similar to pinonaldehyde oxide CI-1b.

28   The SAR-predicted rate coefficient of CI-5b + H_2O is within a factor of 2 of the

29   experimentally derived k_3 value for SCI-A, such that we can equate SCI-A to CI-5b with

30   confidence. The SCI-B set of Criegee intermediates then contains the summed population of

31   the remaining five CI, all of which react slowly with H_2O. The SAR-predicted unimolecular

Atmospheric
Chemistry
and Physics
Discussions

Open Access

EGU

1   decay rate coefficients range from 15 to 700 s^{-1}, all within a factor of 9 of the experimentally

2   obtained k_d = 130 s^{-1}; it should be noted that for limonene-derived CI, no explicit theoretical

3   calculations are available, and the SAR-predictions carry a somewhat larger uncertainty.

4   We have performed an exhaustive characterisation of the conformers of CI-5b. The most

5   stable conformers show an internal complex formation between the oxide moiety and the

6   carbonyl group, similar to those characterized for the bimolecular reaction of CI with

7   carbonyl compounds (Jalan et al., 2013; Wei et al., 2015). The theoretical study by Jiang et al.

8   (2013) on limonene ozonolysis appears to have omitted internal rotation and cannot be

9   compared directly. It seems likely that the limonene-derived CI can thus easily undergo

10   internal SOZ formation, which is thought (Vereecken and Francisco, 2012) to be entropically

11   unfavourable, but to have a low barrier to reaction. For α-pinene, a similar internal complex

12   formation and SOZ ring closure is not as favourable due to the geometric limitations enforced

13   by the 4-membered ring.

14   A large number of transition state conformers for CI-5b + H$_2$O were characterized, though no

15   exhaustive search was completed. The energetically most favourable structures show

16   interaction between the carbonyl group, and the H$_2$O co-reactant as it adds onto the carbonyl

17   oxide moiety. Similar stabilising interactions between the carbonyl moiety and the

18   carbonyl oxide moiety were reported recently in cyclohexene-derived CI

19   (Berndt et al., 2017). This interaction thus lowers the barrier to reaction though it is currently

20   unclear whether it enhances the reaction rate compared to e.g. the α-pinene-derived CI-1b, as

21   these hydrogen-bonded structures are entropically not very favourable. The intra-molecular

22   interactions with heterosubstituents could be investigated in future work.

23

24   **6   Global modelling study**

25   **6.1   SCI Chemistry**

26   A global atmospheric modelling study was performed using the GEOS-Chem chemical

27   transport model (as described in Section 4) to examine the global monoterpene derived SCI

28   budget and the contribution of these SCI to gas-phase SO$_2$ oxidation. The existing chemistry

29   scheme in the model is supplemented with monoterpene SCI chemistry based on the

30   experimental results described in Section 5 and in Table 5. It should be noted here that this

31   modelling study focuses on the chemical impacts of monoterpene SCI formed from

1   ozonolysis reactions only. No chemistry for other SCIs derived from isoprene and/or other

2   (smaller) alkenes are incorporated in the adapted model chemical scheme used.

3   The monoterpene emissions in GEOS-Chem are taken from MEGAN v2.1 (Guenther et al.,

4   2012). The scheme emits seven monoterpenes: α-pinene, β-pinene, limonene, myrcene,

5   ocimene, 3-carene, and sabinene. The monoterpenes are oxidised within the model by OH,

6   NO_3 and O_3 at rates shown in Table S1. Reaction with O_3 leads to the production of

7   monoterpene specific SCI. Reactions with OH and NO_3 does not lead to the formation of any

8   products, with the reactions only acting as a sink for the monoterpene and the respective

9   oxidant. The SCI yields from the ozonolysis of α-pinene, β-pinene, and limonene are derived

10   from the experimental work presented here. SCI from each monoterpene are split in to SCI-A

11   and SCI-B as defined in previous sections. For the other four monoterpenes emitted, the SCI

12   yields, and kinetics are derived based on similarity of structure to one of the species studied

13   here or previously in the literature. The main SCI produced in the ozonolysis of myrcene and

14   ocimene are expected to be acetone oxide $((CH_3)_2COO)$ or 4-vinyl-5-hexenal oxide

15   $(CH_2CHC(CH_2)CH_2CH_2CHOO)$, since ozone has been suggested to react predominantly at

16   the isolated internal double bond (~97 % for myrcene, ~90% for ocimene (Baker et al.,

17   2004)). The SCI yield is taken to be 0.30, similar to that of $(CH_3)_2COO$ from 2,3-dimethyl-

18   but-2-ene ozonolysis (Newland et al., 2015a). However, this may be an underestimate since it

19   has been predicted that stabilisation of small CI increases with an increasing size of carbonyl

20   co-product, as this co-product can take more of the nascent energy of the primary ozonide on

21   decomposition due to a greater number of degrees of freedom available (Nguyen et al., 2009,

22   Newland et al., 2015b). Sabinene is a bicyclic monoterpene with an external double bond and

23   hence is treated like β-pinene. This assumption is backed up by recent theoretical work (Wang

24   and Wang, 2017), who predict similar behaviour of sabinene derived SCI to the predicted

25   behaviour of β-pinene SCI by Nguyen et al. (2009a). They predict a SCI yield between 24 % -

26   64 %. 3-carene is a bicyclic monoterpene with an internal double bond and is treated like α-

27   pinene.

28   **6.2   Modelling Results**

29   Figure 7 shows the annually averaged total SCI burden from monoterpene ozonolysis in the

30   surface layer in the GEOS-Chem simulation. A number of interesting features are apparent

31   from this figure and the associated information given in Table 6:

Atmospheric
Chemistry
and Physics
Discussions

1   (i)   The highest annually averaged monoterpene SCI concentrations are found

2   above tropical forests.

3   (ii)   Peak anually averaged monoterpene SCI concentrations are $\sim 1.2 \times 10^4$ cm^{-3}.

4   (iii)   > 97 % of the total monoterpene SCI burden is SCI-B.

5   Annual global monoterpene emissions are dominated by the tropics (Figure S1), accounting

6   for > 90 % during the northern hemisphere winter months (November – April) and 70 % even

7   during the peak emissions from the northern boreal region during June and July (Sindelarova

8   et al., 2014). Despite annually averaged surface ozone mixing ratios being roughly a factor of

9   2 higher in the northern mid-high latitudes, monoterpene SCI production is still dominated by

10   the tropics. Annually averaged surface monoterpene SCI concentrations across the northern

11   boreal regions are $< 2 \times 10^3$ cm^{-3}; during the summer months (JJA) this value rises to $2 - 5 \times$

12   10^3 cm^{-3}.

13   More than 97 % of the total monoterpene derived SCI are SCI-B (Table 6). This is because

14   typical water vapour concentrations in the tropics are $> 5.0 \times 10^{17}$ cm^{-3}. This gives SCI-A

15   removal rates (i.e. k_3[H$_2$O]) of $2 \times 10^3 - 1.5 \times 10^5$ s^{-1}, whereas removal rates of SCI-B to

16   unimolecular reactions have been determined here to be $1 - 3$ orders of magnitude slower, on

17   the order of 100 - 250 s^{-1}. Since the loss of SCI-B is independent of temperature in the model,

18   the highest SCI-B concentrations would be expected to be located in the regions of highest

19   SCI-B production. Recent experimental studies (Smith et al., 2016) have demonstrated a

20   strong temperature dependence for the unimolecular decomposition rate of (CH$_3$)$_2$COO

21   between 283 and 323 K ($269 - 916$ s^{-1}). Therefore, it may be that in reality there would be

22   some geographical variation in the rate of unimolecular loss.

23   The monoterpene SCI-A + H$_2$O reactions are expected to lead to high yields of both large

24   (e.g. Ma et al., 2008; Ma and Marston, 2008) and small (measured in high yield in the

25   experiments presented here) organic acids.

26   Figure 8 shows the seasonal removal of SO$_2$ by reaction with monoterpene derived SCI, as a

27   percentage of total gas-phase SO$_2$ oxidation in the surface layer. Monoterpene SCI are most

28   important (relative to OH) for SO$_2$ oxidation over tropical forests, where they account for up

29   to 50 % of the local gas-phase SO$_2$ removal during DJF and MAM in some regions. The

30   reasons for this are two-fold: firstly, the highest modelled monoterpene SCI concentrations

31   are found in these regions (Figure 7); but additionally, OH concentrations in the model are

32   low over these areas (Figure S2). Historically there has been discrepancies between modelled

Atmospheric
Chemistry
and Physics
Discussions

1   and observed OH concentrations over tropical forests, with models appearing to under-predict

2   [OH] by up to a factor of ten (e.g. Lelieveld et al., 2008). It was proposed that this was due to

3   missing sources of OH recycling during isoprene oxidation. During recent years there have

4   been advances in our understanding of isoprene chemistry. GEOS-Chem v-09, used here,

5   includes an isoprene OH recycling scheme largely based on Paulot et al. (2009a, 2009b), with

6   updates from Peeters et al. (2009), Peeters and Müller (2010), and Crounse et al. (2011;

7   2012), and evaluated in Mao et al. (2013). However, more recent experimental and theoretical

8   work is not yet included.

9   Annually, monoterpene SCI oxidation accounts for 1.1 % of the gas-phase SO_2 oxidation in

10   the terrestrial tropics. This accounts for the removal of 2.5 Gg of SO_2. Across the northern

11   boreal forests, monoterpene SCI contribute 0.5 % to gas-phase SO_2 removal annually,

12   removing 0.6 Gg of SO_2. Globally, throughout the whole atmosphere, monoterpene SCI

13   account for only 0.4 % of gas-phase SO_2 removal, removing 6.8 Gg of SO_2 annually.

14   It is noted that MEGAN does not contain oceanic monoterpene emissions, which may

15   increase the global importance of SCI for gas-phase SO_2 removal. Luo and Yu (2010)

16   determined annual global oceanic α-pinene emissions to be 29.5 TgC using a top-down

17   approach, with only 0.013 (Luo and Yu, 2010) – 0.26 (Hackenberg et al., 2017) TgC

18   estimated using a range of bottom-up approaches; clearly there are large uncertainties in

19   oceanic monoterpene emissions. At the upper end of this range they could potentially provide

20   a similar contribution to SCI production and subsequent SO_2 oxidation as monoterpenes

21   emitted from the terrestrial biosphere. SCI production more generally could be further

22   amplified by sources such as marine-derived alkyl iodine photolysis.

23   Blitz et al. (2017) recently calculated a revised SO_2 + OH reaction rate (k_1 (1 bar N_2) (298 K)

24   = 5.8 × 10^{-13} cm^3 s^{-1}), based on experimental work and a master equation analysis, which is ~

25   40 % lower than the rate given in the most recent JPL data evaluation (Burkholder et al.,

26   2015) ((k_1 (1 bar N_2) (298 K) = 9.5 × 10^{-13} cm^3 s^{-1}), which is used in the GEOS-Chem model

27   simulation. Figure S3 shows the increased influence of monoterpene derived SCI on gas-

28   phase SO_2 oxidation if the alternative SO_2 + OH rate is used. This increased the impact of

29   monoterpene SCI to up to 60 % of gas-phase SO_2 removal in regions of the tropical forests

30   during DJF and MAM, with the contribution of monoterpene SCI to global gas-phase SO_2

31   oxidation increasing to 0.6 %.

Atmospheric
Chemistry
and Physics
Discussions

1   While certain monoterpenes appear to be more important than others with regard to the

2   production of SCI which will oxidise SO_2, these results are sensitive to the kinetics used and

3   the assumptions made for the monoterpenes not studied experimentally here. Hence we do not

4   attempt to draw any conclusions about the relative importance of each monoterpene from the

5   modelling. Clearly the most important monoterpenes will be those with high yields of SCI-B,

6   particularly if those SCI-B have a structure that hinders unimolecular decomposition (such as

7   certain β-pinene derived SCI).

8

9   **7   Discussion and Atmospheric Implications**

10   Monoterpene ozonolysis produces a diverse range of SCIs, with contrasting fates in the

11   atmosphere, dominated by unimolecular reaction or reaction with water vapour, but which

12   may still affect atmospheric SO_2 processing. Monoterpene-derived SCI have the potential to

13   make a significant contribution to gas-phase SO_2 oxidation in specific local (i.e. forested)

14   environments, of up to 50 % at certain times of year - amplifying sulfate aerosol formation,

15   reducing the atmospheric lifetime and hence geographic distribution of SO_2, however the

16   results presented here show that their impact upon annual SO_2 oxidation globally is modest.

17   The results presented here demonstrate that it is important that monoterpene ozonolysis

18   reactions are considered to produce at least two different SCI species if their chemistry is to

19   be adequately represented in global models. This is because even a 'moderate' reaction rate

20   with water would be a dominant sink of an SCI with the averaged properties of SCI-A and

21   SCI-B.

22   SCI concentrations are expected to vary greatly depending on the local environment and time

23   of year, *e.g.* monoterpene abundance may be considerably higher (and with a different

24   reactive mix of alkenes giving a range of structurally diverse SCI) in a forested environment,

25   compared to a rural background. Furthermore, biogenic isoprene and monoterpene emissions

26   are strongly temperature dependent, hence are predicted to change significantly in the future

27   as a response to a changing climate and other environmental conditions (Peñuelas and Staudt,

28   2010).

29   This study shows that the ozonolysis of monoterpenes may contribute to significant SCI

30   concentrations in forested areas. Another group of compounds produced by forests that may

31   also have the potential to be a significant source of SCI are sesquiterpenes ($C_{15}H_{24}$). Although

1   generally present at low mixing ratios, this is due to their short atmospheric lifetimes caused

2   by their rapid reaction rates with ozone. The flux through the alkene-ozone reaction for fast

3   reacting monoterpenes and sesquiterpenes is often higher than for monoterpenes with high

4   mixing ratios but low removal rates, e.g. α-pinene and β-pinene. Ozonolysis of sesquiterpenes

5   has been shown to have very high SCI yields (Beck et al., 2011; Yao et al., 2014) and these

6   SCI have been shown to react with SCI scavengers (e.g. SO_2, H_2O etc.) in a similar way to

7   smaller SCI (Yao et al., 2014). It has been predicted that SCI from sesquiterpenes may have a

8   high degree of secondary ozonide formation (Chuong et al., 2004) but experimental work has

9   shown very different results for structurally different sesquiterpenes studied (Beck et al.,

10   2011; Yao et al., 2014) hence this is highly uncertain, as is the fate of the SOZ once formed.

11   Therefore, these have the potential to be another significant source of SCI.

12

13   8   Conclusions

14   We report results from an integrated experimental (simulation chamber), theoretical (quantum

15   chemical) and modelling (global chemistry-transport simulation) study of the impacts of

16   monoterpene ozonolysis reactions on stabilised Criegee intermediate (SCI) formation and SO_2

17   oxidation. The ozonolysis of the monoterpenes α-pinene, β-pinene and limonene have been

18   shown to produce a structurally diverse range of chemically distinct SCIs, with some showing

19   limited sensitivity to / reaction with water vapour under near-atmospheric humidity levels. A

20   multi-component system is required to explain the experimentally observed SO_2 removal

21   kinetics. A two-body model system based on the assumption of a fraction of the SCI produced

22   being reactive towards water (SCI-A; potentially contributing to the significant formation of a

23   range of organic acids in the atmosphere), and a fraction being relatively unreactive towards

24   water (SCI-B), analogous to the structural dependencies observed for the simpler CH_3CHOO

25   SCI system, has been shown to describe the observed kinetic data reasonably well for all the

26   monoterpene systems investigated, and may form a computationally affordable and

27   conceptually accessible basis for the description of this chemistry within atmospheric models.

28   The atmospheric fate of SCI-B produced from the monoterpenes studied here will be

29   controlled by their removal by unimolecular decomposition. In this work, we have

30   experimentally determined the monoterpene SCI-B decomposition rate to be between 100 and

31   250 s^{-1}. This has significant implications for the role of monoterpene derived SCI as oxidants

32   in the atmosphere. The fate of SCI-A will be reaction with water or the water dimer, likely

33   leading to the production of a range of organic acids.

Atmospheric
Chemistry
and Physics
Discussions

1 A theory-based analysis of the kinetics of the SCI formed from α-pinene, β-pinene ozonolysis

2 has also been performed, which complements the experimental work. The identification of the

3 likely SCI-A and SCI-B populations and the derived kinetics agree with experimental

4 observations within the respective uncertainties.

5 A modelling study using the GEOS-Chem global 3-D chemical transport model supplemented

6 with the chemical kinetics elucidated in this work suggests that the global monoterpene

7 derived SCI burden will be dominated (> 97%) by SCI-B. The highest annually averaged SCI

8 concentrations are found in the tropics, with seasonally averaged monoterpene SCI

9 concentrations up to 1.2×10^4 cm^{-3} owing to large monoterpene emissions. Across the boreal

10 forest, average SCI concentrations reach between $3 - 5 \times 10^3$ cm^{-3} during the northern

11 hemisphere summer. Oxidation of SO$_2$ by monoterpene SCI is shown to also be most

12 important in the tropics. While oxidation by SCI contributes < 1% to gas-phase SO$_2$ oxidation

13 globally, over tropical forests this can rise to up to 50 % at certain times of the year.

14 Monoterpene SCI driven SO$_2$ oxidation will increase the production of sulfate aerosol –

15 affecting atmospheric radiation transfer, and hence climate; and reduce the atmospheric

16 lifetime and hence transport of SO$_2$. These effects will be substantial in areas where

17 monoterpene emissions are significant, in particular over the Amazon, Central Africa and SE

18 Asian rainforests.

19

20

21 **Data Availability**

24

25 **Acknowledgements**

Atmospheric
Chemistry
and Physics
Discussions

Atmospheric
Chemistry
and Physics
Discussions

Open Access

1 **References**

2 Ahrens, J., Carlsson, P. T. M., Hertl, N., Olzmann, M., Pfeifle, M., Wolf, J. L., and Zeuch, T.:

3 Infrared Detection of Criegee Intermediates Formed during the Ozonolysis of β-pinene and

4 Their Reactivity towards Sulfur Dioxide, Angew. Chem. Int. Ed. Engl., **53**, 715–719, 2014.

5 Alam, M. S., Camredon, M., Rickard, A. R., Carr, T., Wyche, K. P., Hornsby, K. E., Monks,

6 P. S., and Bloss, W. J.: Total radical yields from tropospheric ethene ozonolysis, Phys. Chem.

7 Chem. Phys., 13, 11002–11015, 2011.

8 Alam, M. S., Rickard, A. R., Camredon, M., Wyche, K. P., Carr, T., Hornsby, K. E., Monks,

9 P. S., and Bloss, W. J.: Radical Product Yields from the Ozonolysis of Short Chain

10 Alkenes under Atmospheric Boundary Layer Conditions, J. Phys. Chem. A, 117, 12468-

11 12483, 2013.

12 Anglada, J. M., Gonzalez, J., and Torrent-Sucarrat, M.: Effects of the substituents on the

13 reactivity of carbonyl oxides. A theoretical study on the reaction of substituted carbonyl

14 oxides with water, Phys. Chem. Chem. Phys., 13, 13034–13045, 2011.

15 Anglada, M. and Sole, A.: Impact of the water dimer on the atmospheric reactivity of

16 carbonyl oxides, Phys. Chem. Chem. Phys., 18, 17698-17712, 2016.

17 Asatryan, R. and Bozzelli, J.W.: Formation of a Criegee intermediate in the low-temperature

18 oxidation of dimethyl sulfoxide, Phys. Chem. Chem. Phys., 10, 1769–1780, 2008.

19 Baptista, L., Pfeifer, L., da Silva, E. C., and Arbilla, G.: Kinetics and Thermodynamics of

20 Limonene Ozonolysis, J. Phys. Chem. A, 115, 10911-10919, 2011.

21 Beck, M., Winterhalter, R., Herrmann, F., and Moortgat, G. K.: The gas-phase ozonolysis of

22 α-humulene, Phys. Chem. Chem. Phys., 13, 10970–11001, 2011.

23 Becker, K. H.: EUPHORE: Final Report to the European Commission, Contract EV5V-

24 CT92-0059, Bergische Universität Wuppertal, Germany, 1996.

25 Berndt, T., Voigtländer, J., Stratmann, F., Junninen, H., Mauldin III, R. L., Sipilä, M.,

26 Kulmala, M., and Herrmann, H.: Competing atmospheric reactions of CH_2OO with SO_2 and

27 water vapour, Phys. Chem. Chem. Phys., 16, 19130–19136, 2014.

28 Berndt, T., Kaethner, R., Voigtländer, J., Stratmann, F., Pfiefle, M., Reichle, P., Sipilä, M.,

29 Kulmala, M., and Olzmann, M.: Kinetics of the unimolecular reaction of CH_2OO and the

Atmospheric
Chemistry
and Physics
Discussions

Open Access

EGU

1   bimolecular reactions with the water monomer, acetaldehyde and acetone at atmospheric

2   conditions, Phys. Chem. Chem. Phys., 17, 19862–19873, 2015.

3   Berndt, T., Herrmann, H. and Kurtén, T.: Direct probing of Criegee intermediates from gas-

4   phase ozonolysis using chemical ionization mass spectrometry, J. Am. Chem. Soc., DOI:

5   10.1021/jacs.7b05849, 2017.

6   Berresheim, H., Adam, M., Monahan, C., O'Dowd, C., Plane, J. M. C., Bohn, B., and Rohrer

7   F.: Missing SO_2 oxidant in the coastal atmosphere? – observations from high-resolution

8   measurements of OH and atmospheric sulfur compounds, Atmos. Chem. Phys., 14, 12209-

9   12223, 2014.

10   Bey, I., Jacob, D. J., Yantosca, R. M., Logan, J. A., Field, B. D., Fiore, A. M., Li, Q., Liu, H.

11   Y., Mickley, L. J., and Schultz, M. G.: Global modelling of tropospheric chemistry with

12   assimilated meteorology: Model description and evaluation, J. Geophys. Res., 106, 23073–

13   23095, 2001.

14   Blitz, M. A., Salter, R. J., Heard, D. E., and Seakins, P. J.: An Experimental and Master

15   Equation Study of the Kinetics of OH/OD + SO_2: The Limiting High-Pressure Rate

16   Coefficients, J. Phys. Chem. A, 121, 3184-3191, 2017.

17   J. B. Burkholder, S. P. Sander, J. Abbatt, J. R. Barker, R. E. Huie, C. E. Kolb, M. J. Kurylo,

18   V. L. Orkin, D. M. Wilmouth, and P. H. Wine "Chemical Kinetics and Photochemical Data

19   for Use in Atmospheric Studies, Evaluation No. 18," JPL Publication 15-10, Jet Propulsion

20   Laboratory, Pasadena, 2015 http://jpldataeval.jpl.nasa.gov.

21   Caravan, R. L., Khan, A. H. M., Rotavera, B., Papajak, E., Antonov, I. O., Chen, M. -W., Au,

22   K., Chao, W., Osborn, D. L., Lin, J. J. -M., Percival, C. J., Shallcross, D. E., and Taatjes, C.

23   E.: Products of Criegee intermediate reactions with NO_2: experimental measurements and

24   tropospheric implications, Faraday Discuss., 200, 313-330, 2017.

25   Chao, W., Hsieh, J. -T., Chang, C. -H., and Lin, J. J. -M.: Direct kinetic measurement of the

26   reaction of the simplest Criegee intermediate with water vapour, Science, DOI:

27   10.1126/science.1261549, 2015.

28   Chen, L., Wang, W., Wang, W., Liu, Y., Liu, F., Liu, N., and Wang, B.: Water-catalyzed

29   decomposition of the simplest Criegee intermediate CH_2OO, Theor. Chem. Acc., 135:131,

30   DOI 10.1007/s00214-016-1894-9, 2016.

Atmospheric
Chemistry
and Physics
Discussions

1 Chhantyal-Pun, R., Davey, A., Shallcross, D. E., Percival, C. J., and Orr-Ewing, A. J.: A

2 kinetic study of the CH_2OO Criegee intermediate self-reaction, reaction with SO_2 and

3 unimolecular reaction using cavity ring-down spectroscopy, Phys. Chem. Chem. Phys., 17,

4 3617-3626, 2015.

5 Chhantyal-Pun, R., Welz, O., Savee, J. D., Eskola, A. J., Lee, E. P. F., Blacker, L., Hill, H. R.,

6 Ashcroft, M., Khan, M. A. H. H., Lloyd-Jones, G. C., Evans, L. A., Rotavera, B., Huang, H.,

7 Osborn, D. L., Mok, D. K. W., Dyke, J. M., Shallcross, D. E., Percival, C. J., Orr-Ewing, A. J.

8 and Taatjes, C. A.: Direct Measurements of Unimolecular and Bimolecular Reaction Kinetics

9 of the Criegee Intermediate $(CH_3)_2COO$, J. Phys. Chem. A, 121, 4-15, 2017

10 Chuong, B., Zhang, J, and Donahue, N. M.: Cycloalkene Ozonolysis: Collisionally Mediated

11 Mechanistic Branching, J. Am. Chem. Soc., 126, 12363-12373, 2004.

12 Cox, R. A., and Penkett, S. A.: Oxidation of atmospheric SO_2 by products of the ozone-olefin

13 reaction, Nature, 230, 321-322, 1971.

14 Crounse, J. D., Paulot, F., Kjaergaard, H. G., and Wennberg, P. O.: Peroxy radical

15 isomerization in the oxidation of isoprene, Phys. Chem. Chem. Phys., 13, 13607-13613, 2011.

16 Crounse, J. D., Knap, H. C., Ørnsø, K. B., Jørgensen, S. Paulot, F., Kjaergaard, H. G., and

17 Wennberg, P. O.: Atmospheric fate of methacrolein. 1. Peroxy radical isomerization

18 following addition of OH and O_2, J. Phys. Chem. A., 116, 5756-5762, 2012.

19 Decker, Z. C. J., Au, K., Vereecken, L., and Sheps, L.: Direct experimental probing and

20 theoretical analysis of the reaction between the simplest Criegee intermediate and CH_2OO and

21 isoprene, Phys. Chem. Chem. Phys., 19, 8541-8551, 2017.

22 Donahue, N. M., Drozd, G. T., Epstein, S. A., Presto, A. A., and Kroll, J. H.: Adventures in

23 ozoneland: down the rabbit-hole, Phys. Chem. Chem. Phys., 13, 10848-10857, 2011.

24 Drozd, G. T., and Donahue, N. M.: Pressure Dependence of Stabilized Criegee Intermediate

25 Formation from a Sequence of Alkenes, J. Phys. Chem. A, 115, 4381-4387, 2011.

26 Eckart, C.: The penetration of a potential barrier by electrons, Phys. Rev., 35, 1303-1309,

27 1930.

28 Ehn, M., Thornton, J. A., Kleist, E., Sipilä, M., Junninen, H., Pulli- nen, I., Springer, M.,

29 Rubach, F., Tillmann, R., Lee, B., Lopez- Hilfiker, F., Andres, S., Acir, I.-H., Rissanen, M.,

30 Jokinen, T., Schobesberger, S., Kangasluoma, J., Kontkanen, J., Nieminen, T., Kurtén, T.,

Atmospheric
Chemistry
and Physics
Discussions

1 Nielsen, L. B., Jørgensen, S., Kjaergaard, H. G., Canagaratna, M., Maso, M. D., Berndt,

2 T., Petäjä, T., Wahner, A., Kerminen, V.-M., Kulmala, M., Worsnop, D. R., Wildt, J., and

3 Mentel, T. F.: A large source of low-volatility secondary or- ganic aerosol., Nature, 506, 476–

4 479, doi:10.1038/nature13032, 2014.

5 Fang, Y., Liu, F., Barber, V. P., Klippenstein, S. J., McCoy, A. B. and Lester, M. I.:

6 Communication: Real time observation of unimolecular decay of Criegee intermediates to OH

7 radical products, J. Chem. Phys., 144, 2016a.

8 Fang, Y., Liu, F., Klippenstein, S. J. and Lester, M. I.: Direct observation of unimolecular

9 decay of CH3CH2CHOO Criegee intermediates to OH radical products, J. Chem. Phys., 145,

10 2016b.

11 Fenske, J. D., Hasson, A. S., Ho, A. W., and Paulson, S. E.: Measurement of absolute

12 unimolecular and bimolecular rate constants for CH_3CHOO generated by the trans-2-butene

13 reaction with ozone in the gas phase, J. Phys. Chem. A, 104, 9921–9932, 2000.

14 Foreman, E. S., Kapnas, K. M., and Murray, C.: Reactions between Criegee Intermediates and

15 the Inorganic Acids HCl and HNO3: Kinetics and Atmospheric Implications, Angew. Chem.

16 Int. Ed., 55, 1 – 5, 2016.

17 Frisch, M. J., Trucks, G. W., Schlegel, H. B., Scuseria, G. E., Robb, M. A., Cheeseman, J. R.,

18 Scalmani, G., Barone, V., Mennucci, B., Petersson, G. A., Nakatsuji, H., Caricato, M., Li, X.,

19 Hratchian, H. P., Izmaylov, A. F., Bloino, J., Zheng, G., Sonnenberg, J. L., Hada, M., Ehara,

20 M., Toyota, K., Fukuda, R., Hasegawa, J., Ishida, M., Nakajima, T., Honda, Y., Kitao, O.,

21 Nakai, H., Vreven, T., Montgomery Jr., J. A., Peralta, J. E., Ogliaro, F., Bearpark, M., Heyd,

22 J. J., Brothers, E., Kudin, K. N., Staroverov, V. N., Keith, T., Kobayashi, R., Normand, J.,

23 Normand, J., Raghavachari, K., Rendell, A., Burant, J. C., Iyengar, S. S., Tomasi, J., Cossi,

24 M., Rega, N., Millam, J. M., Klene, M., Knox, J. E., Cross, J. B., Bakken, V., Adamo, C.,

25 Jaramillo, J., Gomperts, R., Stratmann, R. E., Yazev, O., Austin, A. J., Cammi, R., Pomelli,

26 C., Ochterski, J. W., Martin, R. L., Morokuma, K., Zakrzewski, V. G., Voth, G. A., Salvador,

27 P., Dannenberg, J. J., Dapprich, S., Daniels, A. D., Farkas, O., Foresman, J. B., Ortiz, J. V.,

28 Cioslowski, J., Fox, D. J. and Pople, J. A.: Gaussian 09, Revision B.01, Gaussian Inc.,

29 Wallington CT., 2010.

1   Gravestock, T. J., Blitz, M. A., Bloss, W. J., and Heard, D. E.: A multidimensional study of
2   the reaction CH_2I+O_2: Products and atmospheric implications, ChemPhysChem, 11, 3928 –
3   3941, 2010.

4   Guenther, A., Karl, T., Harley, P., Wiedinmyer, C., Palmer, P. I., and Geron, C.: Estimates of
5   global terrestrial isoprene emissions using MEGAN (Model of Emissions of Gases and
6   Aerosols from Nature), Atmos. Chem. Phys., 6, 3181-3210, 2006.

7   Guenther, A. B., Jiang, X., Heald, C. L., Sakulyanontvittaya, T., Duhl, T., Emmons, L. K.,
8   and Wang, X.: The Model of Emissions of Gases and Aerosols from Nature version 2.1
9   (MEGAN2.1): an extended and updated framework for modeling biogenic emissions, Geosci.
10   Model Dev., 5, 1471-1492, 2012.

11   Gutbrod, R., Schindler, R. N., Kraka, E, and Cremer, D.: Formation of OH radicals in the gas
12   phase ozonolysis of alkenes: the unexpected role of carbonyl oxides, Chem. Phys. Lett., 252,
13   221–229, 1996.

14   Hackenberg S. C., Andrews, S. J., Airs, R. L., Arnold, S. R., Bouman, H. A., Cummings, D.,
15   Lewis, A. C., Minaeian, J. K., Reifel, K. M., Small, A., Tarran, G. A., Tilstone, G. H., and
16   Carpenter, L. J.: Basin-Scale Observations of Monoterpenes in the Arctic and Atlantic
17   Oceans, Environ. Sci. Technol., 51, 10449−10458, 2017.

18   Hasson, A. S., Ho, A. W., Kuwata, K. T., and Paulson, S. E.: Production of stabilized Criegee
19   intermediates and peroxides in the gas phase ozonolysis of alkenes 2. Asymmetric and
20   biogenic alkenes, J. Geophys. Res., 106, 34143–34153, 2001.

21   Hatakeyama, S., Kobayashi, H., and Akimoto, H.: Gas-Phase Oxidation of SO_2 in the Ozone-
22   Olefin Reactions, J. Phys. Chem., 88, 4736-4739, 1984.

23   Huang, H. -L., Chao, W., and Lin, J. J. -M.: Kinetics of a Criegee intermediate that would
24   survive at high humidity and may oxidize atmospheric SO_2, Proc. Natl. Acad. Sci., 112,
25   10857–10862, 2015.

26   IUPAC Task Group on Atmospheric Chemical Kinetic Data Evaluation – Data Sheet
27   Ox_VOC20, (http://iupac.pole-ether.fr), 2013.

28   Jalan, A., Allen, J. W., and Green, W. H.: Chemically activated formation of organic acids in
29   reactions of the Criegee intermediate with aldehydes and ketones, Phys. Chem. Chem. Phys.,
30   15, 16841-16852, 2013.

Atmospheric
Chemistry
and Physics
Discussions

1   Jenkin, M. E., Saunders, S. M., and Pilling, M. J.: The tropospheric degradation of volatile

2   organic compounds: a protocol for mechanism development, Atmos. Environ., 31, 81–104,

3   1997.

4   Jenkin, M. E., Young, J. C., and Rickard, A. R.: The MCM v3.3.1 degradation scheme for

5   isoprene, Atmos. Chem. Phys., 15, 11433-11459, 2015.

6   Jiang, L., Lan, R., Xu, Y. -S., Zhang, W. -J., Yang, W.: Reaction of stabilized criegee

7   intermediates from ozonolysis of limonene with water: Ab initio and DFT study, Int. J. Mol.

8   Sci., 14, 5784-5805, 2013.

9   Johnson, D. and Marston, G.: The gas-phase ozonolysis of unsaturated volatile organic

10   compounds in the troposphere, Chem. Soc. Rev., 37, 699–716, 2008.

11   Johnston, H. S. and Heicklen, J.: Tunneling corrections for unsymmetrical Eckart potential

12   energy barriers, J. Phys. Chem., 66, 532–533, 1962.

13   Kidwell, N. M., Li, H., Wang, X., Bowman, J. M., and Lester, M. I.: Unimolecular

14   dissociation dynamics of vibrationally activated CH_3CHOO Criegee intermediates to OH

15   radical products, Nature Chemistry, 8, 509-514, 2016.

16   Kirkby, J., et al.: Ion-induced nucleation of pure biogenic particles, Nature, 533, 521-526,

17   2016.

18   Kjaergaard, H. G., Kurtén, T., Nielsen, L. B., Jørgensen, S., and Wennberg, P. O.: Criegee

19   Intermediates React with Ozone, J. Phys. Chem. Lett., 4, 2525-2529, 2013.

20   Kotzias, D., Fytianos, K., and Geiss, F.: Reactions of monoterpenes with ozone, sulphur

21   dioxide and nitrogen dioxide – Gas phase oxidation of SO_2 and formation of sulphuric acid,

22   Atmos. Environ., 24, 2127-2132, 1990.

23   Kroll, J., Donahue, N. M., Cee, V. J., Demerjian, K. L., and Anderson, J. G.: Gas-phase

24   ozonolysis of alkenes: formation of OH from anti carbonyl oxides, J. Am. Chem. Soc., 124,

25   8518–8519, 2002.

26   Kuwata, K. T., Guinn, E., Hermes, M. R., Fernandez, J., Mathison, J. and Huang, K.: A

27   Computational Re-Examination of the Criegee Intermediate-Sulfur Dioxide Reaction, J. Phys.

28   Chem. A, 119, 10316-10335, 2015.

1   Kuwata, K. T., Hermes, M. R., Carlson, M. J., and Zogg, C. K.: Computational Studies of

2   the Isomerization and Hydration Reactions of Acetaldehyde Oxide and Methyl Vinyl

3   Carbonyl Oxide, J. Phys Chem. A, 114, 9192-9204, 2010.

4   Lelieveld, J., Butler, T. M., Crowley, J. N., Dillon, T. J., Fischer, H., Ganzeveld, L., Harder,

5   H., Lawrence, M. G., Martinez, M., Taraborrelli, D., and Williams, J.: Atmospheric oxidation

6   capacity sustained by a tropical forest, Nature, 452, 737-740, 2008.

7   Leungsakul, S., Jaoui, M., and Kamens, R. M.: Kinetic Mechanism for Predicting Secondary

8   Organic Aerosol Formation from the Reaction of d-limonene with Ozone, Environ. Sci.

9   Technol., 39, 9583-9594, 2005.

10   Lewis, T. R., Blitz, M. A., Heard, D. E., and Seakins, P. W.: Direct evidence for a substantive

11   reaction between the Criegee intermediate, CH_2OO, and the water vapour dimer, Phys. Chem.

12   Chem. Phys., 17, 4859-4863, 2015.

13   Lin, L., Chang, H., Chang, C., Chao, W., Smith, M. C., Chang, C., Lin, J. J., and Takahashi,

14   K.: Competition between H_2O and $(H_2O)_2$ reactions with CH_2OO/CH_3CHOO, Phys. Chem.

15   Chem. Phys., 18, 4557-4568, 2016.

16   Long, B., Bao, J. L. and Truhlar, D. G.: Atmospheric Chemistry of Criegee Intermediates.

17   Unimolecular Reactions and Reactions with Water, J. Am. Chem. Soc., 138, 14409-14422,

18   2016.

19   Luo, G., and Yu, F.: A numerical evaluation of global oceanic emissions of α-pinene and

20   isoprene, Atmos. Chem. Phys., 10, 2007–2015, 2010.

21   Ma, Y., Russell, A. T., and Marston, G.: Mechanisms for the formation of secondary organic

22   aerosol components from the gas-phase ozonolysis of α-pinene, Phys. Chem. Chem. Phys.,

23   10, 4294-4312, 2008.

24   Ma, Y., and Marston, G.: Multi-functional acid formation from the gas-phase ozonolysis of β-

25   pinene, Phys. Chem. Chem. Phys., 10, 6115-6126, 2008.

26   Mao, J., Jacob, D. J., Evans, M. J., Olson, J. R., Ren, X., Brune, W. H., St. Clair, J. M.,

27   Crounse, J. D., Spencer, Beaver, M. R., Wennberg, P. O., Cubison, M. J., Jimenez, J. L.,

28   Fried, A., Weibring, P., Walega, J. G., Hall, S. R., Weinheimer, A. J., Cohen, R. C., Chen, G.,

29   Crawford, J. H., Jaeglé, L., Fisher, J. A., Yantosca, R. M., Le Sager, P., and Carouge,

1   C.: Chemistry of hydrogen oxide radicals (HOx) in the Arctic troposphere in spring, Atmos.
2   Chem. Phys., 10, 5823-5838, 2010.

3   Mao, J., Paulot, F., Jacob, D. J., Cohen, R. C., Crounse, J. D., Wennberg, P. O., Keller, C. A.,
4   Hudman, R. C., Barkley, M. P., and Horowitz, L. W.: Ozone and organic nitrates over the
5   eastern United States: Sensitivity to isoprene chemistry, J. Geophys. Res., 118, 11256–11268,
6   2013.

7   Martinez, R. I., and Herron, J. T.: Stopped-flow studies of the mechanisms of alkene-ozone
8   reactions in the gas-phase: tetramethylethylene, J. Phys. Chem., 91, 946-953, 1987.

9   Mauldin III, R. L., Berndt, T., Sipilä, M., Paasonen, P., Petäjä, T., Kim, S., Kurtén, T.,
10 Stratmann, F., Kerminen, V.-M., and Kulmala, M.: A new atmospherically relevant oxidant,
11 Nature, 488, 193–196, 2012.

12 Newland, M. J., Rickard, A. R., Alam, M. S., Vereecken, L., Muñoz, A., Ródenas, M., and
13 Bloss, W. J.: Kinetics of stabilised Criegee intermediates derived from alkene ozonolysis:
14 reactions with SO_2, H_2O and decomposition under boundary layer conditions, Phys. Chem.
15 Chem. Phys., 17, 4076, 2015a.

16 Newland, M. J., Rickard, A. R., Vereecken, L., Muñoz, A., Ródenas, M., and Bloss, W. J.:
17 Atmospheric isoprene ozonolysis: impacts of stabilised Criegee intermediate reactions with
18 SO_2, H_2O and dimethyl sulfide, Atmos. Chem. Phys., 15, 9521–9536, 2015b.

19 Nguyen, T. L., Peeters, J., and Vereecken, L.: Theoretical study of the gas-phase ozonolysis
20 of β-pinene ($C_{10}H_{16}$), Phys. Chem. Chem. Phys., 11, 5643–5656, 2009a.

21 Nguyen, T. L., Winterhalter, R., Moortgat, G., Kanawati, B., Peeters, J., and Vereecken, L.:
22 The gas-phase ozonolysis of β-caryophyllene ($C_{15}H_{24}$). Part II: A theoretical study, Phys.
23 Chem. Chem. Phys., 11, 4173–4183, 2009b.

24 Nguyen, T. L., Lee, H., Matthews, D. A., McCarthy, M. C. and Stanton, J. F.: Stabilization of
25 the Simplest Criegee Intermediate from the Reaction between Ozone and Ethylene: A High
26 Level Quantum Chemical and Kinetic Analysis of Ozonolysis, J. Phys. Chem. A, 119, 5524-
27 5533, 2015.

28 Niki, H., Maker, P. D., Savage, C. M., Breitenbach, L. P., and Hurley, M. D.: FTIR
29 spectroscopic study of the mechanism for the gas-phase reaction between ozone and
30 tetramethylethylene, J. Phys. Chem., 91, 941–946, 1987.

Atmospheric
Chemistry
and Physics
Discussions

Novelli, A., Vereecken, L., Lelieveld, J., and Harder, H.: Direct observation of OH formation from stabilised Criegee intermediates, Phys. Chem. Chem. Phys., 16, 19941–19951, 2014.

Parrella, J. P., Jacob, D. J., Liang, Q., Zhang, Y., Mickley, L. J., Miller, B., Evans, M. J., Yang, X., Pyle, J. A., Theys, N., and Van Roozendael, M.: Tropospheric bromine chemistry: implications for present and pre-industrial ozone and mercury, Atmos. Chem. Phys., 12, 6723-6740, 2012.

Paulot, F., Crounse, J. D., Kjaergaard, H. G., Kürten, A., Clair, J. M. S., Seinfeld, J. H., and Wennberg, P. O.: Unexpected epoxide formation in the gas-phase photooxidation of isoprene, Science, 325, 730-733, 2009a.

Paulot, F., Crounse, J. D., Kjaergaard, H. G., Kroll, J. H., Seinfeld, J. H., and Wennberg, P. O.: Isoprene photooxidation: New insights into the production of acids and organic nitrates, Atmos. Chem. Phys., 9, 1479-1501, 2009b.

Paulson, S. E., Chung, M., Sen, A. D., and Orzechowska, G.: Measurement of OH radical formation from the reaction of ozone with several biogenic alkenes, Geophys. Res. Lett., 24, 3193–3196, 1997.

Peeters, J., Nguyen, T. L., and Vereecken, L.: HOx radical regeneration in the oxidation of isoprene, Phys. Chem. Chem. Phys., 11, 5935-5939, 2009.

Peeters, J., and Müller, J. F.: HOx radical regeneration in isoprene oxidation via peroxy radical isomerisations. II: Experimental evidence and global impact, Phys. Chem. Chem. Phys., 12, 14227-14235, 2010.

Peñuelas, J., and Staudt, M.: BVOCs and global change, Trends Plant Sci., 15, 133–144, 2010.

Pöschl, U., and Shiraiwa, M.: Multiphase Chemistry at the Atmosphere-Biosphere Interface Influencing Climate and Public Health in the Anthropocene, Chem. Rev., 115, 4440–4475, 2015.

Rickard, A. R., Johnson, D., McGill, C. D., and Marston, G.: OH Yields in the Gas-Phase reactions of Ozone with Alkenes, J. Phys. Chem. A, 103, 7656–7664, 1999.

Rossignol, S., Rio, C., Ustache, A., Fable, S., Nicolle, J., Même, A., D'Anna, B., Nicolas, M., Leoz, E., and Chiappini, L.: The use of a housecleaning product in an indoor environment

leading to oxygenated polar compounds and SOA formation: Gas and particulate phase chemical characterization, Atmos. Environ., 75, 196-205, 2013.

Ryzhkov, A. B., and P. A. Ariya, A theoretical study of the reactions of parent and substituted Criegee intermediates with water and the water dimer, Phys. Chem. Chem. Phys., 6, 5042-5050, 2004.

Sarwar, G., and Corsi, R.: The effects of ozone/limonene reactions on indoor secondary organic aerosols, Atmos. Environ., 41, 959–973, 2007.

Saunders, S. M., Jenkin, M. E., Derwent, R. G., and Pilling, M. J.: Protocol for the development of the Master Chemical Mechanism, MCM v3 (Part A): Tropospheric degradation of non-aromatic volatile organic compounds, Atmos. Chem. Phys., 3, 161-180, 2003.

Shallcross, D. E., Taatjes, C. A., and Percival, C. J.: Criegee intermediates in the indoor environment: new insights, Indoor Air, 24, 495–502, 2014.

Sheps, L., Scully, A. M., and Au, K.: UV absorption probing of the conformer-dependent reactivity of a Criegee intermediate CH_3CHOO Phys. Chem. Chem. Phys., 16, 26701-26706, 2014.

Sindelarova, K., Granier, C., Bouarar, I., Guenther, A., Tilmes, S., Stavrakou, T., Müller, J.-F., Kuhn, U., Stefani, P., and Knorr, W.: Global data set of biogenic VOC emissions calculated by the MEGAN model over the last 30 years, Atmos. Chem. Phys., 14, 9317-9341, 2014.

Singer, B. C., Coleman, B. K., Destaillats, H., Hodgson, A. T., Lunden, M. M., Weschler, C. J., and Nazaroff, W. W.: Indoor secondary pollutants from cleaning product and air freshener use in the presence of ozone, Atmos. Environ., 40, 6696-6710, 2006a.

Singer, B. C., Destaillats, H., Hodgson, A. T., and Nazaroff, W. M.: Cleaning products and air fresheners: emissions and resulting concentrations of glycol ethers and terpenoids, Indoor Air, 16, 179-191, 2006b.

Sipilä, M., Jokinen, T., Berndt, T., Richters, S., Makkonen, R., Donahue, N. M., Mauldin III, R. L., Kurtén, T., Paasonen, P., Sarnela, N., Ehn, M., Junninen, H., Rissanen, M. P., Thornton, J., Stratmann, F., Herrmann, H., Worsnop, D. R., Kulmala, M., Kerminen, V.-M., and Petäjä, T.: Reactivity of stabilized Criegee intermediates (sCIs) from

1   isoprene and monoterpene ozonolysis toward SO_2 and organic acids, Atmos. Chem. Phys., 14,

2   12143-12153, 2014.

3   Smith, M. C., Chao, W., Takahashi, K., Boering, K. A., and Lin, J. J. -M.: Unimolecular

4   Decomposition Rate of the Criegee Intermediate $(CH_3)_2COO$ Measured Directly with UV

5   Absorption Spectroscopy, J. Phys. Chem. A, doi: 10.1021/acs.jpca.5b12124, 2016.

6   Stone, D., Blitz, M., Daubney, L., Howes, N. U. M., and Seakins, P.: Kinetics of CH_2OO

7   reactions with SO_2, NO_2, NO, H_2O, and CH_3CHO as a function of pressure, Phys. Chem.

8   Chem. Phys., 16, 1139-1149, 2014.

9   Su, Y. -T., Lin, H. -Y., Putikam, R., Matsui, H., Lin, M. C., and Lee, Y. -P.: Extremely rapid

10   self-reaction of the simplest Criegee intermediate CH_2OO and its implications in atmospheric

11   chemistry, Nature Chemistry, 6, 477-483, 2014.

12   Taatjes, C. A., Welz, O., Eskola, A. J., Savee, J. D., Osborn, D. L., Lee, E. P. F., Dyke, J. M.,

13   Mok, D. W. K., Shallcross, D. E., and Percival, C. J.: Direct measurements of Criegee

14   intermediate (CH_2OO) formed by reaction of CH_2I with O_2, Phys. Chem. Chem. Phys., 14,

15   10391-10400, 2012.

16   Taatjes, C. A., Welz, O., Eskola, A. J., Savee, J. D., Scheer, A. M., Shallcross, D. E.,

17   Rotavera, B., Lee, E. P. F., Dyke, J. M., Mok, D. K. W., Osborn, D. L., and Percival, C. J.:

18   Direct Measurements of Conformer-Dependent Reactivity of the Criegee Intermediate

19   CH_3CHOO, Science, 340, 177–180, 2013.

20   Taatjes, C. A., Shallcross, D. E., and Percival, C. J.: Research frontiers in the chemistry of

21   Criegee intermediates and tropospheric ozonolysis, Phys. Chem. Chem. Phys., 16, 1704-1718,

22   2014.

23   Taipale, R., Sarnela, N., Rissanen, M., Junninen, H., Rantala, P., Korhonen, F., Siivola, E.,

24   Berndt, T., Kulmala, M., Mauldin, R.L. III, Petäjä, T., Sipilä, M.: New instrument for

25   measuring atmospheric concentrations of non-OH oxidants of SO_2, Bor. Env. Res., 19 (suppl.

26   B), 55-70, 2014.

27   Truhlar, D. G., Garrett, B. C. and Klippenstein, S. J.: Current Status of Transition-State

28   Theory, J. Phys. Chem., 100, 12771-12800, 1996.

1   Vereecken, L. and Peeters, J.: The 1,5-H-shift in 1-butoxy: A case study in the rigorous

2   implementation of transition state theory for a multirotamer system, J. Chem. Phys., 119,

3   5159-5170, 2003.

4   Vereecken, L., and Francisco, J. S.: Theoretical studies of atmospheric reaction mechanisms

5   in the troposphere, Chem. Soc. Rev., 41, 6259-6293, 2012.

6   Vereecken, L., Harder, H., and Novelli, A.: The reaction of Criegee intermediates with NO,

7   RO_2, and SO_2, and their fate in the atmosphere, Phys. Chem. Chem. Phys., 14, 14682–14695,

8   2012.

9   Vereecken, L., Harder, H., and Novelli, A.: The reactions of Criegee intermediates with

10   alkenes, ozone and carbonyl oxides, Phys. Chem. Chem. Phys., 16, 4039–4049, 2014.

11   Vereecken, L., Rickard, A. R., Newland, M. J., and Bloss, W. J.: Theoretical study of the

12   reactions of Criegee intermediates with ozone, alkylhydroperoxides, and carbon monoxide,

13   Phys. Chem. Chem. Phys., 17, 23847–23858, 2015.

14   Vereecken, L., and Nguyen, H. M. T.: Theoretical Study of the Reaction of Carbonyl Oxide

15   with Nitrogen Dioxide: $CH_2OO + NO_2$, Int. J. Chem. Kinet., 49, 752-760, 2017.

16   Vereecken, L.: The Reaction of Criegee Intermediates with Acids and Enols, Phys. Chem.

17   Chem. Phys., DOI: 10.1039/C7CP05132H, 2017.

18   Vereecken, L., Novelli, A., and Taraborrelli, D.: Unimolecular decay strongly limits

19   concentration of Criegee intermediates in the atmosphere, Manuscript in preparation, 2017.

20   Wang, L., and Wang, L.: Mechanism of gas-phase ozonolysis of sabinene in the atmosphere,

21   Phys. Chem. Chem. Phys., doi: 10.1039/c7cp03216a, 2017.

22   Wei, W., Zheng, R., Pan, Y., Wu, Y., Yang, F., and Hong, S.: Ozone Dissociation to

23   Oxygen Affected by Criegee Intermediate, J. Phys. Chem. A, 118, 1644–1650, 2014.

24   Wei, W. -M., Yang, X., Zheng, R. -H., Qin, Y. -D., Wu, Y. -K., Yang, F.: Theoretical studies

25   on the reactions of the simplest Criegee intermediate CH_2OO with CH_3CHO, Comp. Theor.

26   Chem., 1074, 142-149, 2015.

27   Welz, O., Eskola, A. J., Sheps, L., Rotavera, B., Savee, J. D., Scheer, A. M., Osborn, D. L.,

28   Lowe, D., Murray Booth, A., Xiao, P., Anwar H., Khan, M., Percival, C. J., Shallcross, D. E.,

29   and Taatjes, C. A.: Rate coefficients of C1 and C2 Criegee intermediate reactions with formic

Atmospheric
Chemistry
and Physics
Discussions

Open Access

1 and acetic acid near the collision limit: direct kinetics measurements and atmospheric

2 implications, Angew. Chem. Int. Ed. Engl., 53, 4547–4750, 2014.

3 Welz, O., Savee, J. D., Osborn, D. L., Vasu, S. S., Percival, C. J., Shallcross, D. E., and

4 Taatjes, C. A.: Direct Kinetic Measurements of Criegee Intermediate (CH_2OO) Formed by

5 Reaction of CH_2I with O_2, Science, 335, 204–207, 2012.

6 Winterhalter, R., Neeb, P., Grossmann, D., Kolloff, A., Horie, O., and Moortgat, G.: Products

7 and Mechanism of the Gas Phase Reaction of Ozone with β-pinene, J. Atmos. Chem., 35,

8 165-197, 2000.

9 Yao, L., Ma, Y., Wang, L., Zheng, J., Khalizov, A., Chen, M., Zhou, Y., Qi, L., and Cui, F.:

10 Role of stabilized Criegee Intermediate in secondary organic aerosol formation from the

11 ozonolysis of α-cedrene, Atmos. Environ., 94, 448-457, 2014.

12 Zhang, D., and Zhang, R.: Ozonolysis of α-pinene and β-pinene: Kinetics and mechanism, J.

13 Chem. Phys., 122, 114308, 2005.

14 Zhang, J., Huff Hartz, K. E., Pandis, S. N., and Donahue, N. M.: Secondary Organic Aerosol

15 Formation from Limonene Ozonolysis: Homogeneous and Heterogeneous Influences as a

16 Function of NO_x, J. Phys. Chem. A, 110, 11053-11063, 2006.

17 Zhou, L., Gierens, R., Sogachev, A., Mogensen, D., Ortega, J., Smith, J. N., Harley, P. C.,

18 Prenni, A. J., Levin, E. J. T., Turnipseed, A., Rusanen, A., Smolander, S., Guenther, A. B.,

19 Kulmala, M., Karl, T., and Boy, M.: Contribution from biogenic organic compounds to

20 particle growth during the 2010 BEACHON-ROCS campaign in a Colorado temperate needle

21 leaf forest, Atmos. Chem. Phys. Discuss., 15, 9033-9075, doi:10.5194/acpd-15-9033-2015,

22 2015.

23

24

25

Atmospheric
Chemistry
and Physics
Discussions

Open Access

EGU

1   Table 1. Monoterpene SCI yields derived in this work and reported in the literature.

ϕ_{SCI}	Reference	Notes	Methodology
α-pinene			
0.19 (± 0.01)	This work		SO_2 loss
0.15 (± 0.07)	Sipilä et al. (2014)		Formation of H_2SO_4
0.22	Taipale et al. (2014) (personal comm. Berndt)		
0.125 (± 0.04)	Hatakeyama et al. (1984)		Formation of H_2SO_4
0.20	MCMv3.3.1 [a]		
β-pinene			
0.60 (± 0.03)	This work		SO_2 loss
0.46	Ahrens et al. (2014)	ϕ_{C9-SCI}: 0.36 ϕ_{CH2OO}: 0.10	FTIR detection
0.25	MCMv3.3.1 [a]	ϕ_{C9-SCI}: 0.102 ϕ_{CH2OO}: 0.148	
0.42	Nguyen et al. (2009)	ϕ_{C9-SCI}: 0.37 ϕ_{CH2OO}: 0.05	Theoretical
0.51	Winterhalter et al. (2000)	ϕ_{C9-SCI}: 0.35 ϕ_{CH2OO}: 0.16	Change in nopinone yields $f([H_2O])$
0.44	Kotzias et al. (1990)		Formation of H_2SO_4
0.25	Hatakeyama et al. (1984)		Formation of H_2SO_4
0.30	Zhang and Zhang (2005)	ϕ_{C9-SCI}: 0.22 ϕ_{CH2OO}: 0.08	
> 0.27	Ma and Marston (2008)	ϕ_{C9-SCI}: 0.27 ϕ_{CH2OO}: 0.16[a] ϕ_{CH2OO}: 0.06[b]	Change in nopinone yields $f([H_2O])$
0.27	Hasson et al. (2001)		Change in nopinone yields $f([H_2O])$
Limonene			
0.23 (± 0.01)	This work		SO_2 loss
0.27 (± 0.12)	Sipilä et al. (2014)		Formation of H_2SO_4
0.34	Leungsakul et al. (2005)	$\phi_{C10-SCI}$: 0.26 ϕ_{CI-x}: 0.04 ϕ_{CH2OO}: 0.05	Measurement of stable particle and gas-phase products
0.135	MCMv3.3.1 [a]		

Atmospheric
Chemistry
and Physics
Discussions

Open Access

EGU

1 Uncertainty ranges (± 2σ, parentheses) indicate combined precision and systematic measurement error

2 components for this work, and are given as stated for literature studies. All referenced experimental studies

3 produced SCI from MT + O_3 and were conducted between 700 and 760 Torr. [a] http://mcm.leeds.ac.uk/MCM/

4 (Jenkin et al., 2015).

5 [a] assuming 100 % stabilisation

6 [b] assuming 40 % stabilisation

1   Table 2. Monoterpene derived SCI relative and absolute[a] rate constants derived in this work.

SCI	$10^5\ k_3/k_2$	$10^{15}\ k_3$ ($cm^3\ s^{-1}$)	$10^{-12}\ k_d/k_2$ (cm^{-3})	k_d (s^{-1})
α-pinene				
SCI-A	> 140 (± 34)	> 310 (± 75)[a]		
SCI-B			< 8.2 (± 1.5)	< 240 (± 44)[c]
β-pinene				
SCI-A	> 10 (± 2.7)	> 4 (± 1)[b]		
SCI-B			< 6.0 (± 1.3)	< 170 (± 38)[c]
Limonene				
SCI-A	< 3.5 (± 0.2)	< 7.7 (± 0.6)[a]		
SCI-B			> 4.5 (± 0.1)	> 130 (± 3)[c]

2   Uncertainty ranges (± 2σ, parentheses) indicate combined precision and systematic measurement error

3   components. [a] Scaled to an absolute value using k_2(anti-CH_3CHOO) = 2.2 × 10^{-10} cm^3 s^{-1} (Sheps et al., 2014); [b]

4   Scaled to an absolute value using k_2(anti-CH_3CHOO) = 4 × 10^{-11} cm^3 s^{-1} (Ahrens et al., 2014); [c] Scaled using

5   k_2(syn-CH_3CHOO) = 2.9 × 10^{-11} cm^3 s^{-1} (Sheps et al., 2014).

6

7

8

9

10

11

12

13

1 Table 3. Unimolecular reactions for the CI derived from α-pinene, β-pinene, and *d*-limonene,

2 as derived by Vereecken et al. (2017). Barrier heights (kcal mol^{-1}) listed estimate post-

3 CCSD(T) energies.

Carbonyl oxide	Reaction	E_b	k(298K) / s^{-1}
α-pinene			
CI-1a	1,4-H-migration	15.8	600
	SOZ-formation	15.6	5×10^{-2}
	1,3-ring closure	21.6	1×10^{-3}
CI-1b	1,3-ring closure	14.8	60
	1,3-H-migration	29.0	1×10^{-6}
CI-2a	1,4-H-migration	16.3	250
	1,3-ring closure	20.8	6×10^{-3}
CI-2b	1,4-H-migration	17.0	60
	SOZ-formation	13.5	8
	Ring closure	19.9	3×10^{-2}
β-pinene			
CI-3	1,4-H-migration	15.7	375
	1,3-ring closure	21.1	2×10^{-3}
CI-4	1,3-ring closure	17.2	2.0
	Ring opening	23.6	(Slow, Nguyen et al. 2009a)
	1,4-H-migration	24.9	(Slow, Nguyen et al. 2009a)
CH$_2$OO	1,3-ring closure	19.0	0.3
	1,3-H-migration	30.7	1×10^{-7}
Limonene[a]			
CI-5a	1,4-H-migration	SAR	200 [a]
CI-5b	1,3-ring closure	SAR	75 [a]
CI-6a	1,4-H-migration	SAR	430 [a]
CI-6b	1,4-H-migration	SAR	700 [a]
CI-7a	1,4-H-migration	SAR	15
CI-7b	1,4-H-migration	SAR	600

4 [a] Formation of secondary ozonides (SOZ) is not included, and could be the dominant unimolecular loss.

5

6

Atmospheric
Chemistry
and Physics
Discussions

1 Table 4. Rate coefficients (cm^3 molecule^{-1} s^{-1}) for the reaction of CI with H_2O and $(H_2O)_2$ as

2 predicted by Vereecken et al. (2017). Values are based on explicit CCSD(T)/aug-cc-

3 pVTZ//M06-2X/aug-cc-pVTZ calculations and multi-conformer TST, including empirical

4 corrections to reference experimental data, except for limonene-derived CI where the values

5 are predicted using a structure-activity relationship. The rate coefficients for CH_2OO,

6 CH_3CHOO, and $(CH_3)_2COO$ are within a factor of 4 of evaluated literature data (Vereecken et

7 al., 2017).

Carbonyl oxide	k(298K) H_2O	k(298K) $(H_2O)_2$
CH_2OO	8.7×10^{-16}	1.4×10^{-12}
syn-CH_3CHOO	6.7×10^{-19}	2.1×10^{-15}
anti-CH_3CHOO	2.3×10^{-14}	2.7×10^{-11}
$(CH_3)_2COO$	7.5×10^{-18}	1.8×10^{-14}
α-pinene		
CI-1a	1.3×10^{-18}	2.9×10^{-15}
CI-1b	1.5×10^{-14}	1.7×10^{-11}
CI-2a	1.0×10^{-18}	2.5×10^{-15}
CI-2b	2.4×10^{-19}	7.0×10^{-16}
β-pinene		
CI-3	1.7×10^{-18}	4.3×10^{-15}
CI-4	4.2×10^{-16}	6.4×10^{-13}
Limonene		
CI-5a	1.5×10^{-18}	4.3×10^{-15}
CI-5b	1.5×10^{-14}	1.7×10^{-11}
CI-6a	9.1×10^{-18}	2.1×10^{-14}
CI-6b	1.5×10^{-17}	3.2×10^{-14}
CI-7a	9.7×10^{-18}	1.9×10^{-14}
CI-7b	4.3×10^{-18}	1.1×10^{-14}

8

9

1   Table 5. Kinetic parameters used in the global modelling study.

SCI	ϕ_{SCI}	$10^{15}\,k_3$ (cm^3 s^{-1})	$10^{11}\,k_2$ [a] (cm^3 s^{-1})	k_d (s^{-1})
α-pinene				
SCI-A	0.08	310	22	-
SCI-B	0.11	-	2.9	240
β-pinene				
SCI-A	0.25	4	4	-
SCI-B	0.35	-	2.9	170
Limonene				
SCI-A	0.05	7.7	22	-
SCI-B	0.18	-	2.9	130
Myrcene				
SCI-B	0.30	-	13[b]	819[c]
Ocimene				
SCI-B	0.30	-	13[b]	819[c]
Sabinene [d]				
SCI-A	0.25	4	4	-
SCI-B	0.35	-	2.9	170
3-carene [e]				
SCI-A	0.08	310	22	-
SCI-B	0.11	-	2.9	240

2   [a] k_2(SCI-A+SO$_2$) from (SO$_2$+*anti*-CH$_3$CHOO) - Sheps et al. (2014); k_2(SCI-B+SO$_2$) from (SO$_2$+*syn*-CH$_3$CHOO)
3   - Sheps et al. (2014) unless otherwise stated
4   [b] k_2(SCI-B+SO$_2$) from (SO$_2$+*anti*-(CH$_3$)$_2$COO) – Huang et al. (2015)
5   [c] k_d(SCI-B) from Newland et al. (2015) (scaled to k_2(SCI-B+SO$_2$) from Huang et al. (2015)
6   [d] Kinetics based on β-pinene
7   [e] Kinetics based on α-pinene
8

1   Table 6. Monoterpene contribution to [SCI] and SO_2 oxidation in the surface layer of the
2   model simulation.

Monoterpene	Annual emissions[a] (Tg C)	% contribution to [SCI-A]	% contribution to [SCI-B]	% contribution to SO_2 oxidation
α-pinene	35.4	0.5	16	6.9
β-pinene	16.9	74	46	65
limonene	9.2	3.5	14	7.2
myrcene	3.1	0.0	1.2	4.5
trans-β-ocimene	14.1	0.0	5.4	11
sabinene	7.9	22	14	4.5
3-carene	6.4	0.0	2.7	1.6

3   [a] From MEGAN v2.1 (Guenther et al., 2012)
4

Atmospheric
Chemistry
and Physics
Discussions

Open Access

1
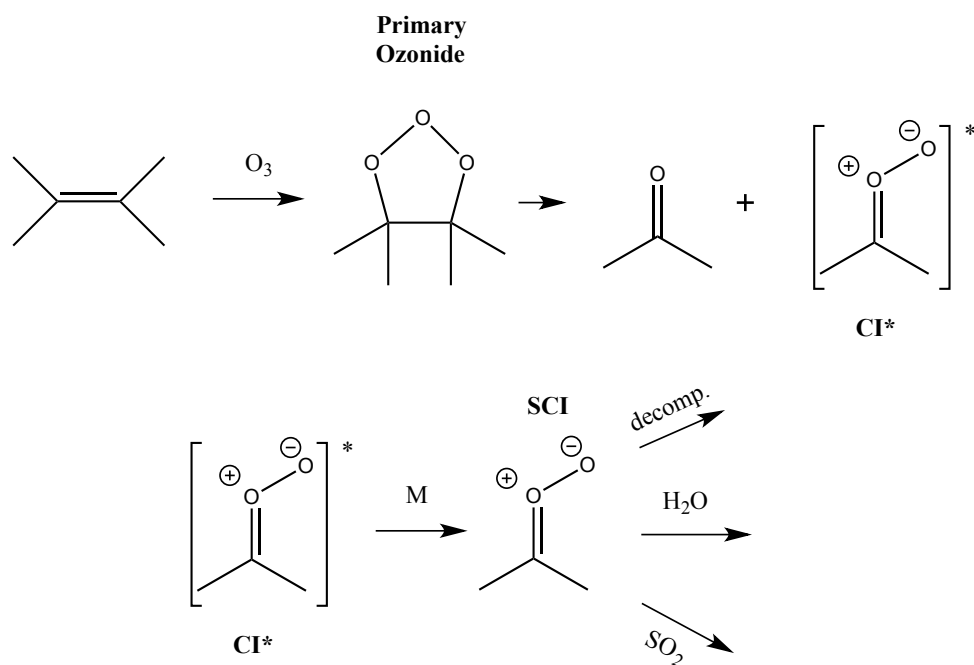
3 Scheme 1. Simplified generic mechanism for the reaction of Criegee Intermediates (CIs)

4 formed from alkene ozonolysis.

5

6

7

8

9

10

11

12

13

14

15

Atmospheric
Chemistry
and Physics
Discussions
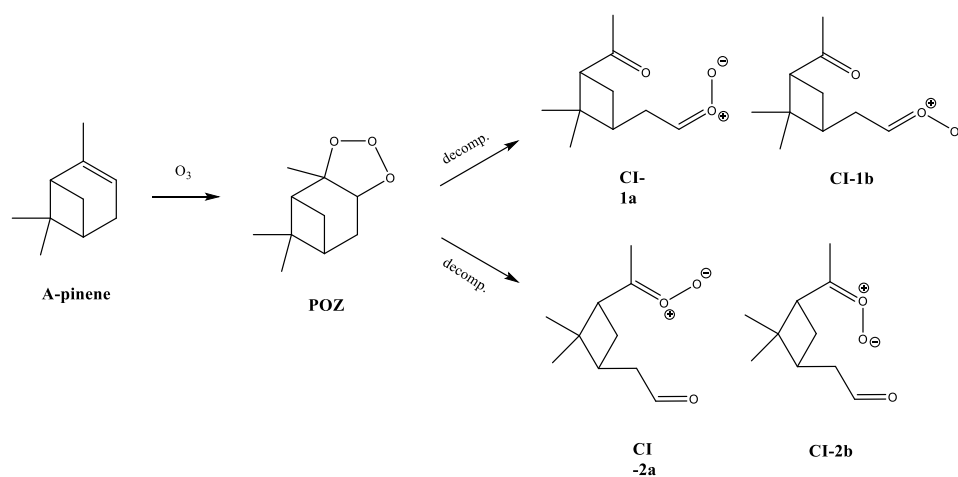
1

2

3   Scheme 2. Mechanism of formation of the two Criegee Intermediates (CIs) from α-pinene

4   ozonolysis.

5

6

7

8

9

10
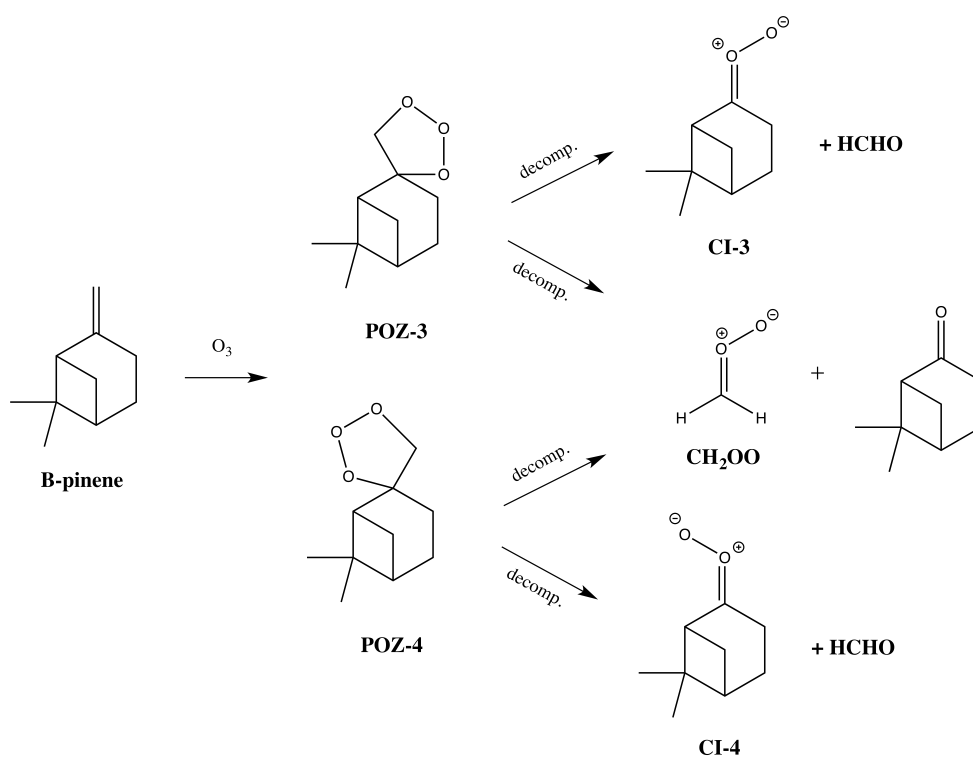
1

2

3   Scheme 3. Mechanism of formation of the three Criegee Intermediates (CIs) from β-pinene

4   ozonolysis.

Atmospheric
Chemistry
and Physics
Discussions

Open Access
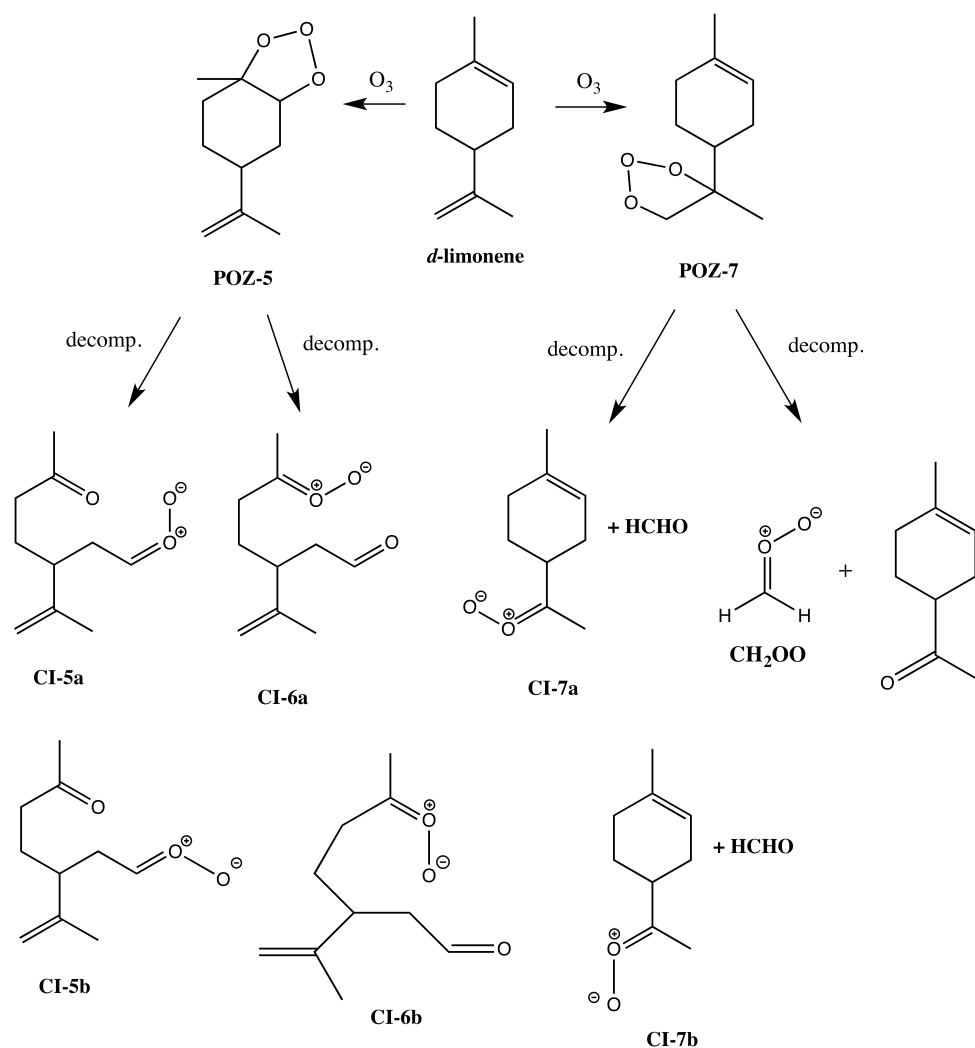
1

2

3   Scheme 4. Mechanism of formation of the four Criegee Intermediates (CIs) from limonene

4   ozonolysis.

5

1
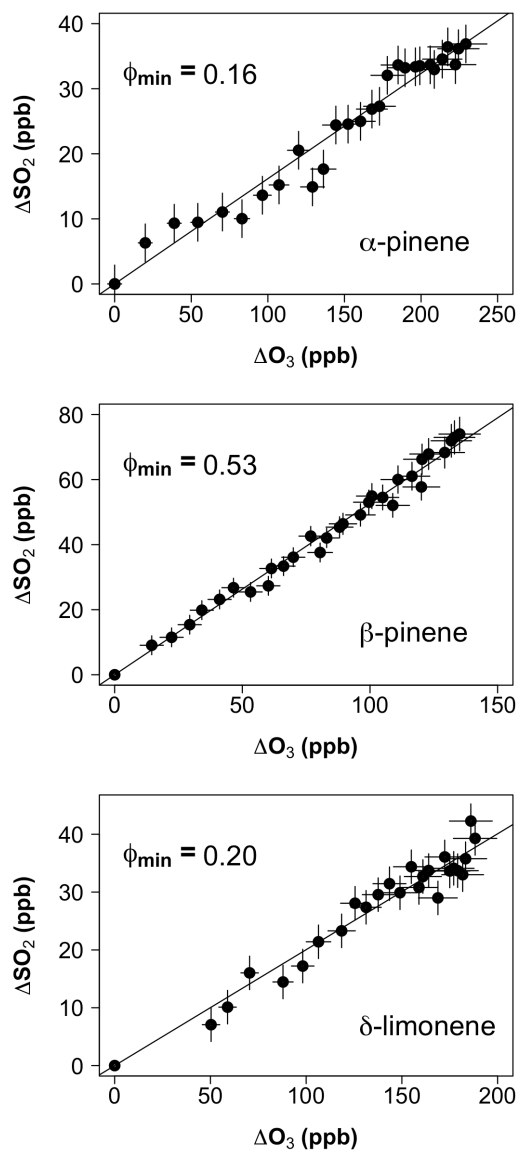
2 Figure 1. ΔSO_2 vs. ΔO_3 during excess SO_2 experiments ($[H_2O] < 5 \times 10^{15}$ cm^{-3}). The gradient

3 determines the minimum SCI yield (ϕ_{min}).

4

Atmospheric
Chemistry
and Physics
Discussions

Open Access

EGU
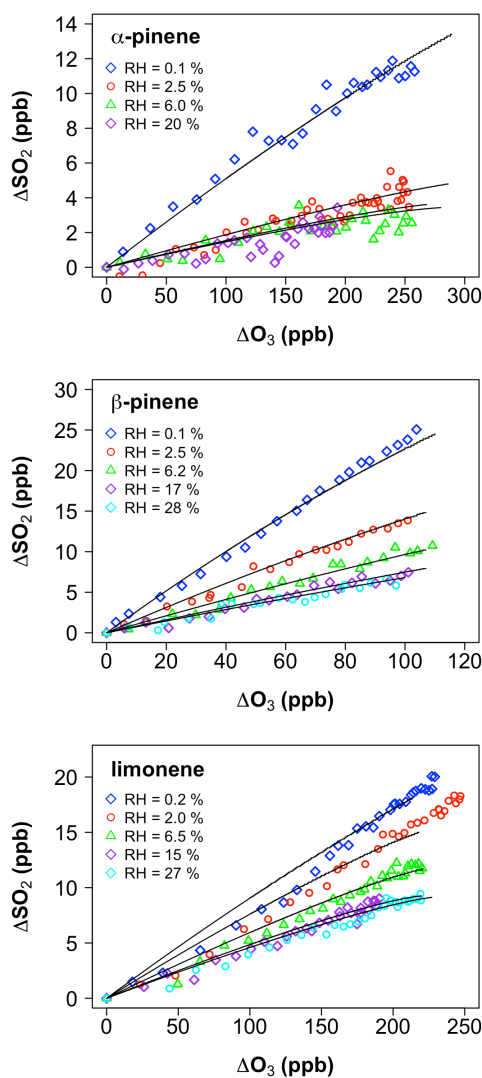
1

2   Figure 2. Cumulative consumption of SO_2 as a function of cumulative consumption of O_3,

3   ΔSO_2 versus ΔO_3, for the ozonolysis of α-pinene, β-pinene and limonene in the presence of

4   SO_2 at a range of water vapour concentrations, from 1×10^{15} cm^{-3} to 1.9×10^{17} cm^{-3}. Symbols

5   are experimental data, corrected for chamber dilution. Lines are smoothed fits to the

6   experimental data.
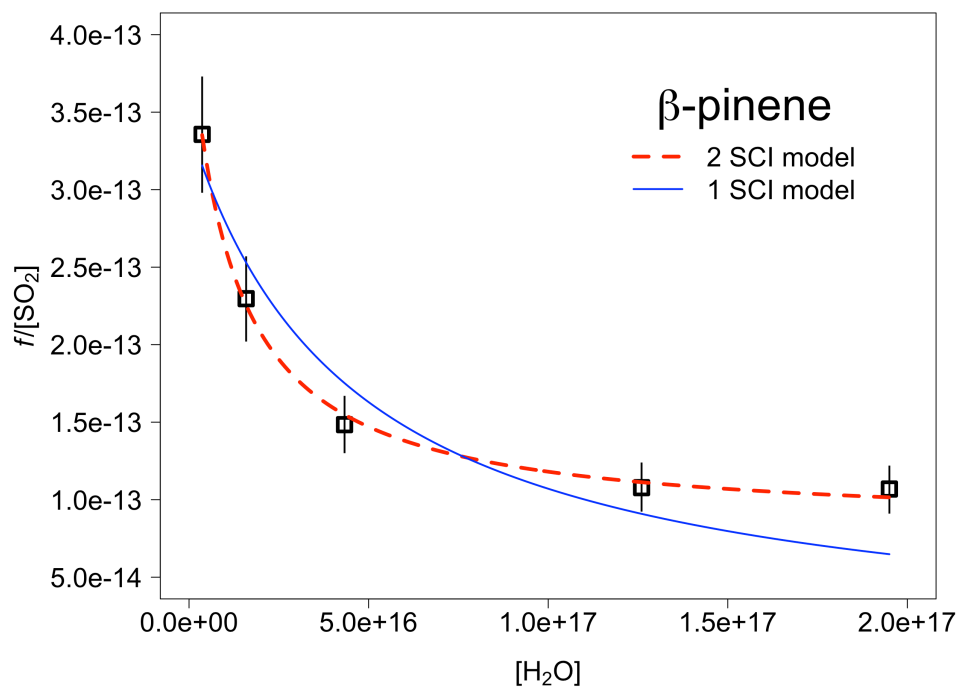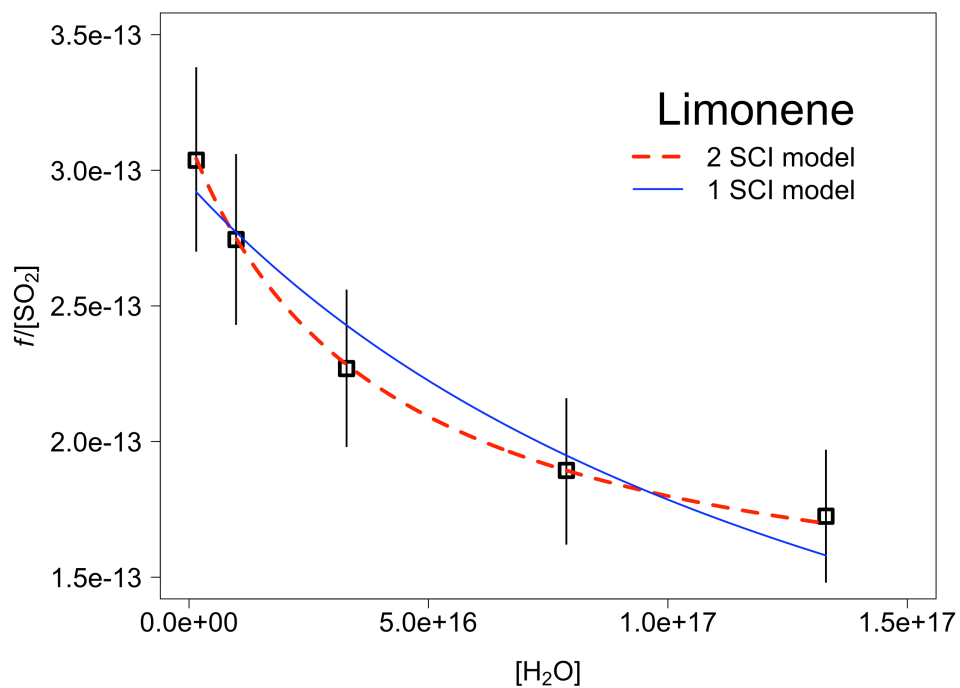
7
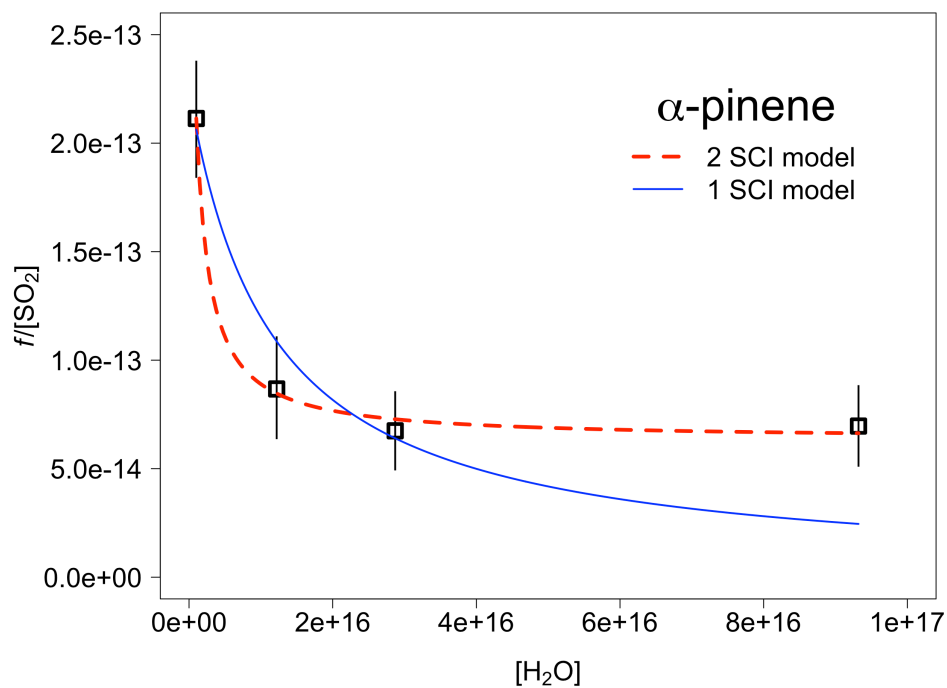
1

2 Figure 3. Application of a 2 SCI model fit (Equation E4) and a single SCI model fit (Equation

3 E1) to the measured values (open squares) of f/[SO$_2$] for α-pinene. From the fit we derive

4 relative rate constants for reaction of the α-pinene derived SCI, SCI-A and SCI-B with H$_2$O

5 (k_3/k_2) and decomposition ((k_d+L)/k_2) assuming that $\gamma^A = 0.40$ and $\gamma^B = 0.60$.

6

7

8

9

10

Atmospheric
Chemistry
and Physics
Discussions

1

2   Figure 4. Application of a 2 SCI model fit (Equation E4) and a single SCI model fit (Equation

3   E1) to the measured values (open squares) of f/[SO_2] for β-pinene. From the fit we derive

4   relative rate constants for reaction of the β-pinene derived SCI, SCI-A and SCI-B with H_2O

5   (k_3/k_2) and decomposition ((k_d+L)/k_2) assuming that $\gamma^A = 0.41$ and $\gamma^B = 0.59$.

1

2

3 Figure 5. Application of a 2 SCI model fit (Equation E4) and a single SCI model fit (Equation

4 E1) to the measured values (open squares) of $f/[SO_2]$ for limonene. From the fit we derive

5 relative rate constants for reaction of the limonene derived SCI, SCI-A and SCI-B with H_2O

6 (k_3/k_2) and decomposition $((k_d+L)/k_2)$ assuming that $\gamma^A = 0.22$ and $\gamma^B = 0.78$.
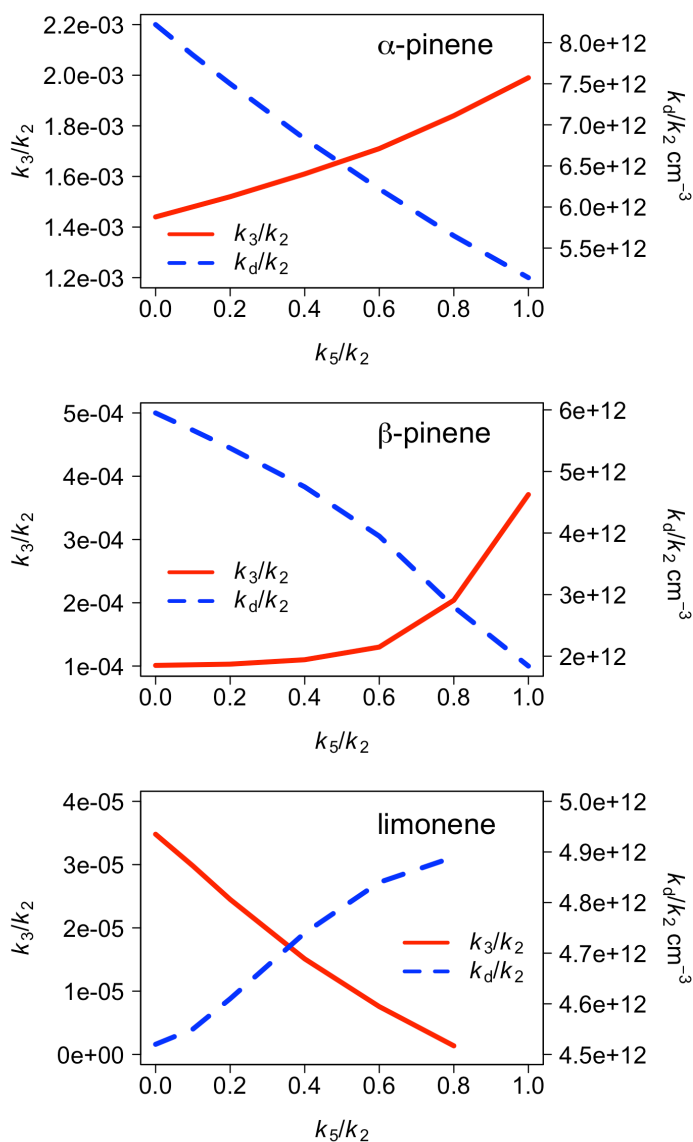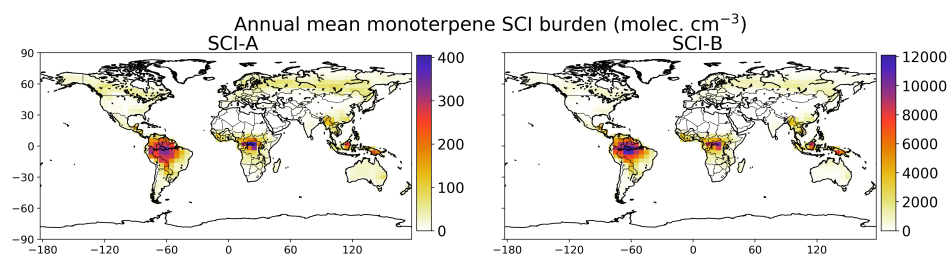
7

8

9

10

11

12

13

Atmospheric
Chemistry
and Physics
Discussions

Open Access

EGU

1

2   Figure 6. Variation of k_3/k_2 (k(SCI-A+H_2O))/(k(SCI-A+SO_2)) and k_d (k(SCI-B
3   unimol.))/(k(SCI-B+SO_2)) as a function of the ratio k_5/k_2 (k(SCI+acid)/k(SCI+SO_2)), derived
4   from least squares fit of Equation E4 to measurements shown in Figures 3 -5 for α-
5   pinene, β-pinene and limonene respectively.

6

7

Figure 7. Annual mean monoterpene SCI-A and SCI-B concentrations (cm^{-3}) in the surface layer of the GEOS-Chem simulation.

Atmospheric
Chemistry
and Physics
Discussions
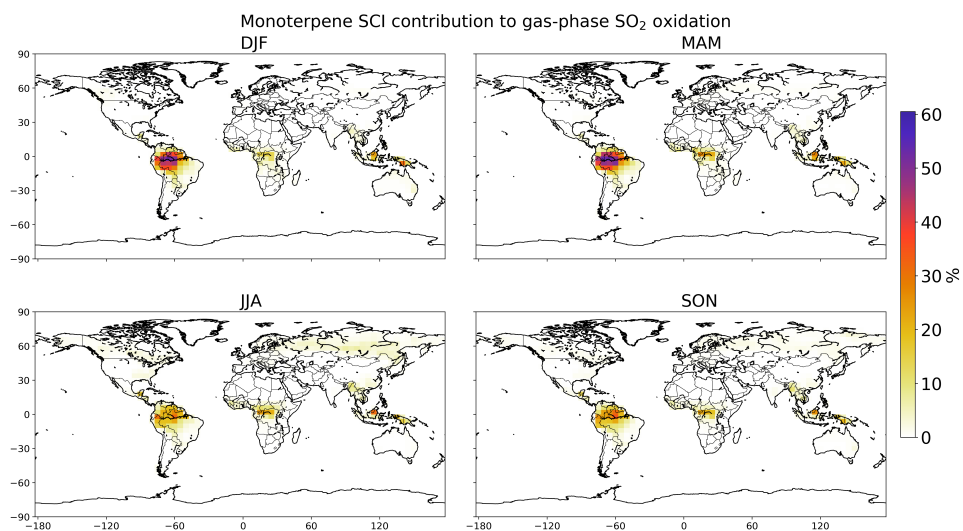
Figure 8. Seasonal SO_2 oxidation by monoterpene SCI as percentage of total gas-phase SO_2 oxidation in the surface layer.